






















# Barley *Mla3* recognizes the host-specificity effector *Pwl2* from *Magnaporthe oryzae*

Helen J. Brabham <sup>1,2,†</sup> Diana Gómez De La Cruz <sup>1,†</sup> Vincent Were <sup>1</sup> Motoki Shimizu <sup>3</sup> Hiromasa Saitoh <sup>4</sup> Inmaculada Hernández-Pinzón <sup>1</sup> Phon Green <sup>1</sup> Jennifer Lorang <sup>5</sup> Koki Fujisaki <sup>3</sup> Kazuhiro Sato <sup>6</sup> István Molnár <sup>7,‡</sup> Hana Šimková <sup>7</sup> Jaroslav Doležel <sup>7</sup> James Russell <sup>1</sup> Jodie Taylor <sup>1</sup> Matthew Smoker <sup>1</sup> Yogesh Kumar Gupta <sup>1,2</sup> Tom Wolpert <sup>5</sup> Nicholas J. Talbot <sup>1</sup> Ryohei Terauchi <sup>3,8</sup> and Matthew J. Moscou <sup>1,\*§</sup>

- 1 The Sainsbury Laboratory, University of East Anglia, Norwich Research Park, Norwich NR4 7UH, UK
- 2 Blades, Evanston, IL 60201, USA
- 3 Iwate Biotechnology Research Centre, Kitakami 024-0003, Japan
- 4 Department of Molecular Microbiology, Tokyo University of Agriculture, Tokyo 156-8502, Japan
- 5 Department of Botany and Plant Pathology, Oregon State University, Corvallis, OR 97331, USA
- 6 Institute of Plant Science and Resources, Okayama University, Kurashiki 710-0046, Japan
- 7 Institute of Experimental Botany of the Czech Academy of Sciences, 779 00 Olomouc, Czech Republic
- 8 Laboratory of Crop Evolution, Graduate School of Agriculture, Kyoto University, Kyoto 617-0001, Japan

\*Author for correspondence: matthew.moscou@usda.gov

<sup>†</sup>These authors contributed equally.

<sup>‡</sup>Present address: Agricultural Institute, Centre for Agricultural Research, ELKH, Martonvásár 2462 Hungary.

<sup>§</sup>Present address: USDA-ARS, Cereal Disease Laboratory, St. Paul, MN 55108, USA.

The author responsible for distribution of materials integral to the findings presented in this article in accordance with the policy described in the Instructions for Authors (<https://academic.oup.com/plcell/pages/General-Instructions>) is Matthew J. Moscou (matthew.moscou@usda.gov).

## Abstract

Plant nucleotide-binding leucine-rich repeat (NLRs) immune receptors directly or indirectly recognize pathogen-secreted effector molecules to initiate plant defense. Recognition of multiple pathogens by a single NLR is rare and usually occurs via monitoring for changes to host proteins; few characterized NLRs have been shown to recognize multiple effectors. The barley (*Hordeum vulgare*) NLR gene *Mildew locus a* (*Mla*) has undergone functional diversification, and the proteins encoded by different *Mla* alleles recognize host-adapted isolates of barley powdery mildew (*Blumeria graminis* f. sp. *hordei* [Bgh]). Here, we show that *Mla3* also confers resistance to the rice blast fungus *Magnaporthe oryzae* in a dosage-dependent manner. Using a forward genetic screen, we discovered that the recognized effector from *M. oryzae* is Pathogenicity toward Weeping Lovegrass 2 (*Pwl2*), a host range determinant factor that prevents *M. oryzae* from infecting weeping lovegrass (*Eragrostis curvula*). *Mla3* has therefore convergently evolved the capacity to recognize effectors from diverse pathogens.

## Introduction

Plants are routinely exposed to a diverse array of microbes, and their interaction is governed by active processes that recognize self and nonself molecular patterns. The plant immune system comprises membrane-localized extracellular receptors and intracellular receptors that detect pathogen molecules or

host-derived molecules generated during pathogen infection (Jones and Dangl 2006). Plant pathogens secrete effector molecules to promote virulence through manipulation of the host environment and suppression of the plant immune system. Effectors are highly sequence and structurally diverse molecules, evolving to evade plant recognition while maintaining virulence function (Franceschetti et al. 2017).

## IN A NUTSHELL

**Background:** Nucleotide-binding leucine-rich repeat (NLR) proteins are intracellular immune receptors that recognize molecules from plant pathogens, known as effectors. The majority of NLRs confer resistance to 1 pathogen by recognizing a specific effector. In barley (*Hordeum vulgare*), the *Mla* locus contains multiple NLR genes, and alleles of the NLR *Mla* recognize *Blumeria graminis*, the causal agent of powdery mildew. In the barley cultivar Baronesse, resistance to the blast pathogen *Magnaporthe oryzae* has been mapped to the *Mla* locus, but the causal gene within this locus is unknown.

**Question:** How is the barley cultivar Baronesse resistant to multiple pathogens? Which gene in the *Mla* locus provides resistance to the rice blast pathogen? Does the *Mla* allele *Mla3* in Baronesse recognize *M. oryzae* in addition to *B. graminis*? What effector is being recognized from *M. oryzae*?

**Findings:** We show that the barley NLR MLA3 recognizes the effector Pwl2 from *M. oryzae*. Resistance to blast disease was mapped to the *Mla* locus. Three candidate genes were cloned and introduced into a susceptible barley cultivar. Infection assays with *M. oryzae* in transgenic barley lines found that only barley carrying *Mla3* showed resistance and required multiple copies. To identify the *M. oryzae* effector recognized by *Mla3*, mutants were generated by randomly knocking genes out in *M. oryzae* using UV mutagenesis. Sequencing mutants found that the effector gene *PWL2* was always lost. *PWL2* was first discovered in 1995, as it prevents blast isolates from infecting weeping lovegrass (*Eragrostis curvula*). MLA3 was shown to directly recognize and associate with Pwl2 through expression and protein–protein assays.

**Next steps:** The main question that remains to be addressed is how does MLA3 recognize *M. oryzae* and *B. graminis*? Future efforts will involve finding the molecular principles of Pwl2 recognition by MLA3 and identifying the recognized effector of *B. graminis* to understand the mechanism by which MLA3 recognizes multiple pathogens.

Nucleotide-binding leucine-rich repeat (NLR) proteins are the largest class of immune receptors in plants and are grouped by their variable N-terminal domains: coiled coil (CC), Toll, interleukin-1 receptor, resistance protein (TIR), or RESISTANCE TO POWDERY MILDEW 8 (RPW8) domain (Ngou et al. 2022). The majority of characterized NLRs recognize single species- or isolate-specific effectors, initiating immune signaling and plant defense upon recognition (Kourelis and van der Hoorn 2018).

The mechanism of recognition by NLRs is broadly classified by the direct and indirect perception of pathogen-derived molecules (Kourelis and van der Hoorn 2018; Saur et al. 2021). Direct recognition involves physical interaction of the NLR and effector to initiate NLR activation (direct model) (Jia et al. 2000), whereas indirect recognition by NLRs occurs through monitoring host targets or guardees for effector-mediated modifications (guard model) (Van Der Biezen and Jones 1998). Host targets can also become integrated into NLRs within the same ORF via fusion events, forming additional domains for effector interaction and recognition (integration model) (Cesari et al. 2014; Cesari 2018). These NLRs with integrated domains routinely require a second NLR to initiate defense signaling (Cesari et al. 2014; Cesari 2018). Extensive functional analysis has been performed on NLRs from each of these modes of recognition; however, the evolution and maintenance of these diverse recognition mechanisms are complex and often unclear (Märkle et al. 2022).

The majority of characterized NLRs confer resistance to 1 pathogen species or recognize single effectors present in

pathogen populations. Across plant species, recognition of the same effectors or host targets can be conferred by orthologous NLRs or by unrelated NLRs through convergent evolution. For example, the host protein kinase AVRPPHB SUSCEPTIBLE 1 (PBS1) is guarded by unrelated NLRs in *Arabidopsis thaliana*, barley (*Hordeum vulgare*), and soybean (*Glycine max*), which convergently recognize the bacterial effector AvrPphB-induced modifications of PBS1 (Caldwell and Michelmore 2009; Kim et al. 2016; Sun et al. 2017; Carter et al. 2019; Helm et al. 2019). RPM1 INTERACTING PROTEIN 4 (RIN4) is another example of a conserved guarded component of the plant immune system. The *A. thaliana* NLRs RESISTANCE TO P. SYRINGAE PV MACULICOLA 1 (RPM1) and RESISTANT TO P. SYRINGAE 2 (RPS2) (Mackey et al. 2002; Axtell and Staskawicz 2003; Mackey et al. 2003; Kim et al. 2005, 2009), soybean Resistance to *Pseudomonas glycinea* 1b (Rpg1b) and Resistance to *Pseudomonas glycinea* 1r (Rpg1r) (Ashfield et al. 2004, 2014; Russell et al. 2015), and wild apple (*Malus × robusta*) *Malus × robusta* 5 (Mr5) (Prokhorchik et al. 2020) all recognize RIN4 perturbation by pathogen effectors. Overall, convergent recognition of effectors by distinct NLRs commonly requires monitoring conserved host targets.

In contrast, recognition of multiple pathogens by single NLRs is rare. Reported cases include the NLR HOPZ-ACTIVATED RESISTANCE 1 (ZAR1) from *A. thaliana*, which recognizes the effector AvrAC from *Xanthomonas campestris*, and HopZ1a and HopF2a from *Pseudomonas syringae* by guarding the receptor-like cytoplasmic kinases PBS1-LIKE 2 (PBL2), RESISTANCE RELATED KINASE 1 (RKS1), HOPZ-ETI DEFICIENT (ZED), and ZED1-RELATED

KINASE 3 (ZRK3) (Lewis et al. 2013; Wang et al. 2015; Seto et al. 2017). The paired NLRs RESISTANT TO RALSTONIA SOLANACEARUM 1 (RRS1)/RESISTANT TO *P. SYRINGAE* 4 (RPS4) recognize the effectors Pop2 and AvrRps4 from the bacterial pathogens *Ralstonia solanacearum* and *P. syringae*, respectively, and an unknown effector from the fungal pathogen *Colletotrichum higginsianum*. Recognition of Pop2 and AvrRps4 is mediated by the integrated WRKY domain at the C-terminus of RRS1 through direct binding and also acetylation by Pop2 (Williams et al. 2014; Le Roux et al. 2015; Sarris et al. 2015; Saucet et al. 2015; Ma et al. 2018; Mukhi et al. 2021). The tomato (*Solanum lycopersicum*) NLR Mi-1 confers resistance against taxonomically divergent pathogens including root-knot nematodes (*Meloidogyne* spp.), potato aphid (*Macrosiphum euphorbiae*), and sweet potato whiteflies (*Bemisia* spp.) (Vos et al. 1998; Nombela et al. 2003; Goggin et al. 2006; Santos et al. 2020). Mi-1 requires the helper NLR NRC4 for cell death signaling, but the molecular mechanism of pathogen recognition remains unknown. Lastly, *Mla8* in barley confers resistance to barley powdery mildew (*Blumeria graminis* f. sp. *hordei*) and wheat stripe rust (*Puccinia striiformis* f. sp. *tritici*) (Bettgenhaeuser et al. 2021). Interestingly, MLA8 does not contain an integrated domain, and no interacting partner NLRs have yet been implicated for functional resistance.

The barley *Mla* locus on the short arm of chromosome 1H is a resistance gene complex showing extreme intraspecific diversity in barley haplotypes (Briggs and Stanford 1938; Jørgensen and Wolfe 1994; Zhou et al. 2001; Wei et al. 2002; Seeholzer et al. 2010). Characterization of the *Mla* locus in the reference genome Morex identified a complex region containing 3 NLR gene families—*RGH1* (*Mla*), *RGH2*, and *RGH3*—that are located in 3 gene-rich regions flanked by repetitive and mobile elements (Wei et al. 2002). Allelic variants of the *Mla* CC-NLR gene (*RGH1*) confer isolate-specific immunity against the host pathogen barley powdery mildew *Bgh* (Jørgensen and Wolfe 1994; Kinizios et al. 1995; Halterman et al. 2001; Seeholzer et al. 2010). The LRR region of *Mla* determines recognition specificity and shows signatures of positive selection (Shen et al. 2003; Halterman and Wise 2004; Seeholzer et al. 2010; Maekawa et al. 2019). A direct recognition mechanism for MLA has been proposed, shown by the direct interaction between MLA1, MLA7, MLA10, MLA13, and MLA22 and the *Bgh* effectors AVR<sub>a1</sub>, AVR<sub>a7</sub>, AVR<sub>a10</sub>, AVR<sub>a13</sub>, and AVR<sub>a22</sub>, respectively (Lu et al. 2016; Saur et al. 2019; Bauer et al. 2021).

Recognition of diverse pathogens has been genetically linked to the *Mla* locus including susceptibility to *Bipolaris sorokiniana* (Reaction to *Cochliobolus sativus* 6 [Rcs6]) (Bilgic et al. 2006; Leng et al. 2018, 2020) and resistance to *Magnaporthe oryzae* (syn. *Pyricularia oryzae*; Reaction to *Magnaporthe oryzae* 1 [Rmo1]) (Inukai et al. 2006). Previous work found that *Rmo1* was in genetic coupling with the *Mla* locus in the barley accession Baronesse (*Mla3*) (Inukai et al. 2006). In this study, we find that *Rmo1* is in complete genetic coupling with *Mla3* through performing a high-resolution recombination screen. Using RNA-seq, RenSeq-PacBio, and chromosome sequencing, we

show that all 3 NLR gene families at the *Mla3* locus—*RGH1*, *RGH2*, and *RGH3*—are present and expressed in Baronesse. We report that Baronesse carries 4 near-identical copies of *Mla3* (*RGH1*). Characterization of a diversity panel and *Mla* introgression lines suggested that *Mla3* underlies *Rmo1*-mediated resistance. *Agrobacterium*-mediated transformation provides evidence that *Mla3* (*RGH1*) specifically confers resistance to *M. oryzae* isolate KEN54-20 (AVR-*Rmo1*) in a dosage-dependent manner. Using association genetics and mutagenesis combined with high-throughput sequencing, we report the unexpected finding that MLA3 (RMO1) recognizes the known host species specificity determinant Pwl2 (AVR-*Rmo1*) from *M. oryzae*.

## Results

### *Mla3* is in complete genetic coupling with *Rmo1*

To elucidate the genetic relationship of *Mla3* and *Rmo1*, a recombination screen using a Baronesse × BCD47 F<sub>2</sub> population ( $N = 2,304$  gametes) was performed over a wide 22.9 cM region on chromosome 1H encompassing the *Mla* locus (markers K\_3\_1144 and K\_2\_0712) (Fig. 1). Among 169 recombinants, 80 recombinants were identified between the flanking markers of the *Mla* locus (K\_963924 and K\_206D11). Marker saturation of the region encompassing *Mla* was performed using 12 Kompetitive allele specific PCR (KASP) markers spanning a wide genetic interval from markers K\_3\_0933 to K\_4261. Homozygous recombinants were identified for 53 F<sub>2:3</sub> families. Suppressed recombination was observed at the *Mla3* locus, with 18 markers in complete genetic coupling with K\_Mla\_RGH1, that spans a ~240 kb physical region in the reference sequence cv. Morex (Wei et al. 2002). The marker K\_Mla\_RGH1 was designed on a single nucleotide polymorphism (SNP) between *Mla3* coding sequence and the *RGH1* allele in BCD47 (*RGH1*-BCD47).

To determine if the marker K\_Mla\_RGH1 is in coupling with barley powdery mildew (*Bgh*) resistance, recombinants within the interval surrounding the *Mla3* locus were phenotyped with *Bgh* isolate CC148 (AVR<sub>a3</sub>). Using these 165 F<sub>2:3</sub> families, resistance to *Bgh* isolate CC148 cosegregated with marker K\_Mla\_RGH1. Baronesse and BCD47 show clear differential phenotypes upon inoculation with the *M. oryzae* isolate KEN54-20 carrying AVR-*Rmo1*. To map *Rmo1*, 42 homozygous F<sub>2:4</sub> families with recombination events near the *Mla* locus were inoculated with *M. oryzae* isolate KEN54-20 using leaf spot inoculation (Fig. 1B) and whole plant spray inoculation (Fig. 1C). Resistance to *M. oryzae* isolate KEN54-20 cosegregated with marker K\_Mla\_RGH1. Therefore, *Rmo1* is in complete genetic coupling with *Mla3*.

### *Mla3* (*RGH1*), *RGH2*, and *RGH3* are present and expressed in the *Mla3* haplotype from Baronesse

In the reference genome Morex, the *Mla* locus includes multiple members of 3 CC-NLR gene families—*RGH1*, *RGH2*, and *RGH3*—of which all 3 are present within a 40 kb tandem duplication (Wei et al. 1999, 2002). Due to high repetitive

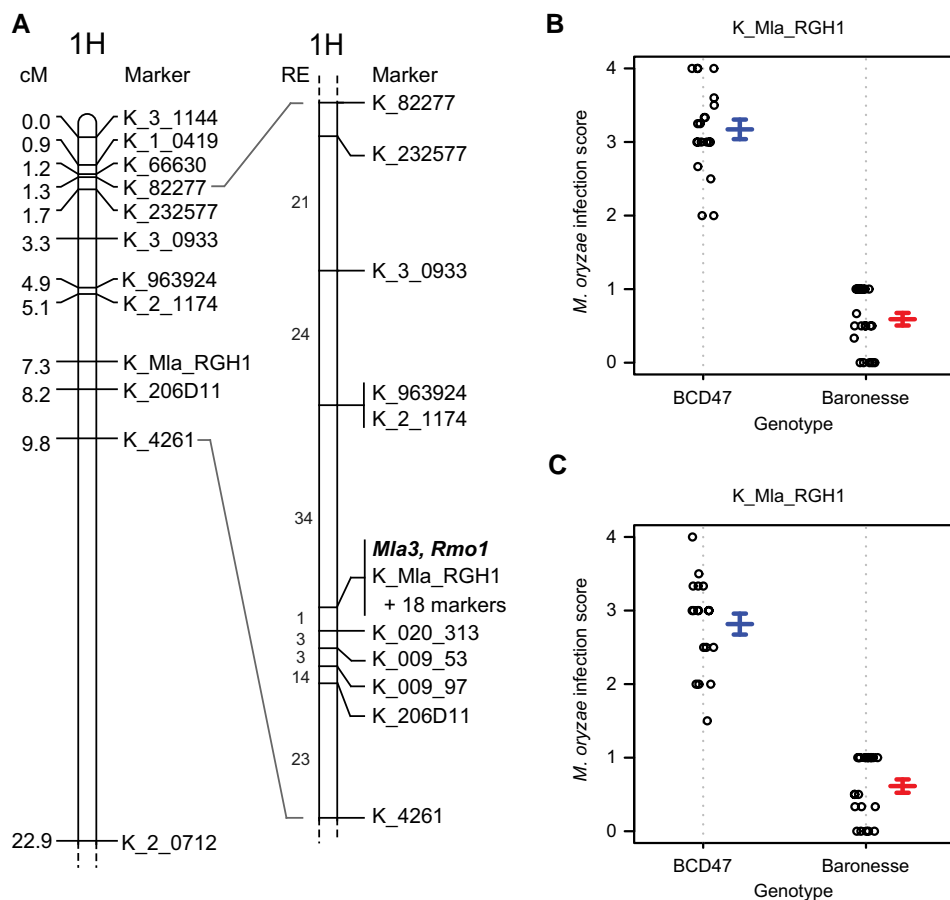


**Figure 1.** *Rmo1* is in complete coupling with *Mla3*. **A**) The distal end of the short arm of chromosome 1H based on nonredundant KASP markers in the Baronesse × BCD47 population (2,304 gametes). RE, number of recombination events between markers. Twenty additional markers (not shown) are in complete genetic coupling with K\_Mla\_RGH1\_2920 at the *Mla* locus. **B**) Phenotype by genotype plot of homozygous F<sub>2:4</sub> recombinants inoculated with *M. oryzae* isolate KEN54-20 using a spot-based inoculation. Scores 0 and 1 = resistant and 2 to 4 = susceptible. **C**) Phenotype by genotype plot of homozygous F<sub>2:4</sub> recombinants inoculated with *M. oryzae* isolate KEN54-20 using a spray-based inoculation. Scores 0 and 1 = resistant and 2 to 4 = susceptible.

content and presence of large near-identical duplications, the *Mla* locus fails to assemble correctly using short-read sequencing technology (Mascher et al. 2021). We therefore used several approaches to resolve the genomic region encompassing *Mla3*.

Using chromosome flow sorting and Chicago long-range linkage (Thind et al. 2017), we assembled chromosome 1H from barley accession Baronesse. Genomic scaffolds were fragmented at the boundaries of the *Mla* locus, with the distal and proximal regions defined by scaffold1235 and scaffold1874, respectively (Fig. 2; Supplemental Fig. S1). Genomic sequence of *Mla3* (RGH1) was fragmented, with fragments found on scaffold1874 and 3 small contigs (contigs 38,297, 42,637, and 63,307), whereas RGH2 and RGH3 were found to be in a head-to-head orientation on scaffold1874. The flanking intervals for the *Mla3* haplotype are highly colinear with the Morex haplotype (Fig. 2A; Supplemental Fig. S1). Using a complementary approach, we applied RenSeq-PacBio (Witek et al. 2016) with a capture library designed on NLRs that included baits designed on *Mla3* (RGH1),

RGH2, and RGH3 gene families (Brabham et al. 2018). *Mla3* and RGH2/RGH3 were assembled on 15.3 and 14.0 kb contigs, respectively (Fig. 2B).

We hypothesized that the fragmented assembly is due to repetitive gene content or large near-identical duplications, such as observed in the reference genome (Mascher et al. 2021). To identify potential duplications, we used *k*-mer counting with flow-sorted chromosome 1H sequencing data using genomic contigs encompassing *Mla3* and RGH2/RGH3 identified by RenSeq-PacBio as template (Fig. 3). Based on local regression of *k*-mer coverage, the single copy gene *Barley Pumilio/Mpt5/BBF-like* (*Bpm*) located immediately proximal to the *Mla* locus had an estimated coverage of 161.6 (5' region) and 165.1 (3' region) (Fig. 3A), whereas *Mla3* had an estimated coverage of 800.1 (Fig. 3B). Evaluation of individual *k*-mer coverage found that the average coverage is an overestimate due to high-copy *k*-mers present in the central region of *Mla3*. Analysis using *k*-medoids found that individual *k*-mers of *Mla3* clustered at 146, 619, and 790, corresponding to 1, 4, and 5 copies, respectively

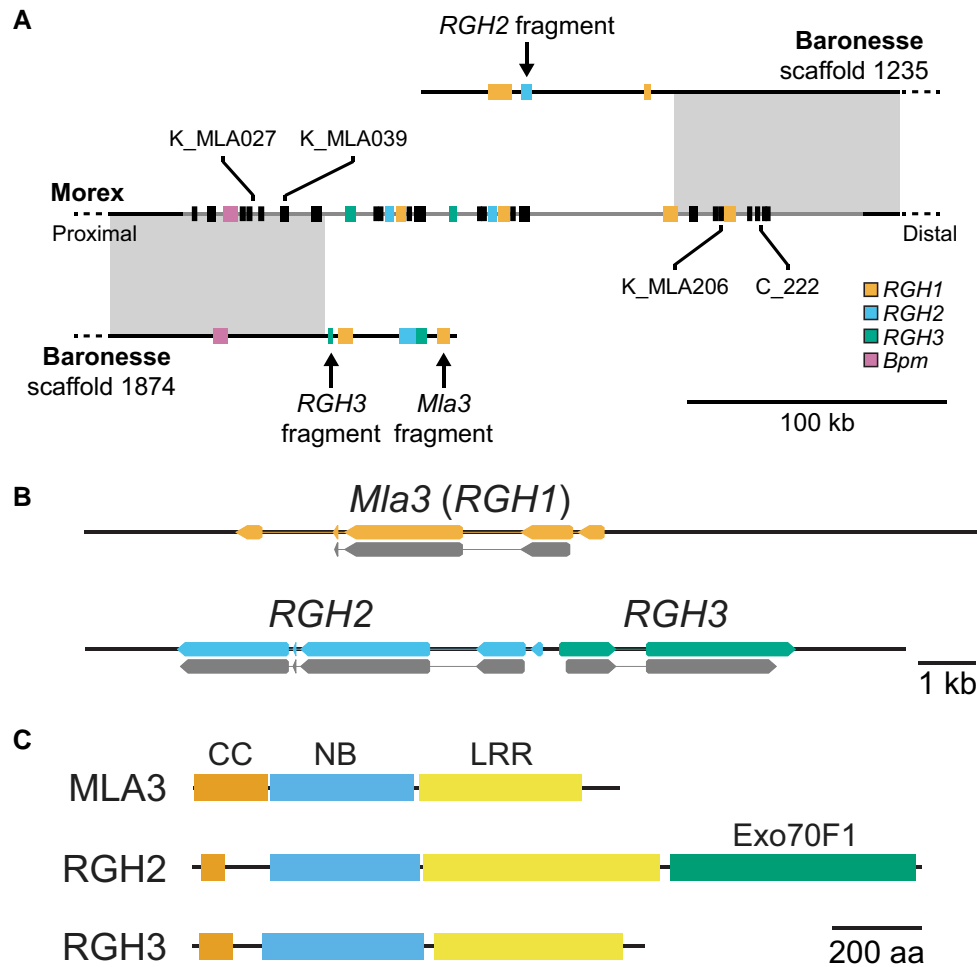


**Figure 2.** The *Mla* locus in Baronesse is highly divergent in sequence and structure. **A**) Sequence alignment of the region encompassing *Mla* in barley accessions Morex (*mla*) and Baronesse (*Mla3*) found high conservation in the flanking intervals (left and right boxes) but no conservation within the *Mla* locus. The central region of *Mla* is a breakpoint in the assembly of chromosome 1H from barley accession Baronesse. *RGH1*, *RGH2*, and *RGH3* family members are indicated in orange, blue, and green, respectively. KASP and CAPS markers are indicated with "K\_" and "C\_" prefixes, respectively. **B**) RenSeq-PacBio identified genomic contigs encompassing *Mla3* (15.3 kb) and *RGH2*/*RGH3* (14.0 kb). In the barley accession Baronesse haplotype, *RGH2* and *RGH3* are in head-to-head orientation. **C**) In the barley accession Baronesse haplotype, *Mla3* and *RGH3* encode CC-NB-LRR, whereas *RGH2* encodes an CC-NB-LRR with integrated Exo70F1.

(Supplemental Fig. S2). The same approach found *Bpm* and *RGH2*/*RGH3* had *k*-medoids of 175 ( $k = 1$ ) and 162 and 315 ( $k = 2$ ), respectively (Supplemental Fig. S2). *RGH2* and *RGH3* are single copy, although fragments of the C-terminal encoding regions of the NLRs are present in scaffolds 1235 and 1874, respectively, that flank the *Mla* locus (Figs. 2A and 3C). For *Mla3*, *k*-mers contributing to 5 copies are concentrated in the regions encoding the CC and nucleotide-binding (NB) domains (Fig. 3B). Two regions in the leucine-rich repeat region of *Mla3* were found to have a reduction in *k*-mer coverage suggesting that a single copy of *Mla3* had diverged from other copies (Fig. 3B). Evaluation of aligned genomic reads found heterogeneity in *Mla3* copies, with 1 copy carrying a 6 base pair deletion resulting in 2 deletions and 1 change in the amino acid sequence. This copy was designated *Mla3Δ6*. Collectively, based on this analysis, we conclude that Baronesse carries 3

identical copies of *Mla3*, *Mla3Δ6*, and an *RGH1* family member that is diverged from *Mla3*.

De novo transcriptome assembly of RNA-seq from first leaf of Baronesse found that *Mla3*, *RGH2*, and *RGH3* family members were expressed. To confirm expression of the *Mla3Δ6* copy and identify other expressed variants, we aligned RNA-seq onto gene models of *Mla3*, *RGH2*, and *RGH3*. No variation was found in *RGH2* and *RGH3*, whereas we verified the existence of 2 expressed variants of *Mla3* (*Mla3* and *Mla3Δ6*). Baronesse *RGH2* encodes an NLR with an integrated Exo70F1 and is in head-to-head orientation with *RGH3* (Fig. 2C). *RGH2* and *RGH3* belong to the Major Integration Clade 1 (MIC1) and C7 clades of NLRs, respectively (Bailey et al. 2018; Brabham et al. 2018). Other members of the MIC1 clade include *Rpg5* from barley (Wang et al. 2013) and *RGA5* from rice (*Oryza sativa*) (Cesari et al. 2014), which require additional NLRs to function as a pair. Their respective

partners, *RGA1* (Wang et al. 2013) and *RGA4* (Cesari et al. 2014), also reside in the C7 clade. Following this observation, we hypothesize that *RGH2* and *RGH3* also function as paired NLRs. Therefore, candidate genes for conferring *Rmo1* resistance are *Mla3*, *Mla3Δ6*, and the paired NLRs *RGH2* and *RGH3*.

### Baronesse *RGH2* and *RGH3* do not confer *Rmo1*-mediated resistance

An Exo70 in rice, OsExo70F3, is the target of the *M. oryzae* effector AVR-Pii, and this interaction is guarded by the resistance gene pair *Pii-1* and *Pii-2* (Fujisaki et al. 2015). We hypothesized that Exo70s could be a conserved effector target between rice and barley; hence, *RGH2* and *RGH3* are candidates for conferring *Rmo1*-mediated resistance. Barley haplotypes contain extensive variation at the *Mla* locus (Seeholzer et al. 2010; Brabham et al. 2018; Maekawa et al. 2019). To leverage this natural variation, we investigated *RGH2* and *RGH3* in a panel of over 40 diverse barley accessions de novo assembled transcriptomes (Supplemental Data Set 1) (Brabham et al. 2018; Maekawa et al. 2019). We identified multiple accessions containing diverse allelic variants of *RGH2* and *RGH3*. Of these, the accession Maritim contains identical copies of *RGH2* and *RGH3* as found in the accession Baronesse but carries a divergent *Mla* allele. Screening the diversity panel with *M. oryzae* isolate KEN54-20 (*AVR-Rmo1*) using both a spray- and spot-based inoculation found that all accessions, aside from Baronesse, were susceptible (Fig. 4; Supplemental Fig. S3). Therefore, we conclude that *RGH2* and *RGH3* do not confer *Rmo1*-mediated resistance.

### *Mla3* is *Rmo1*

To assess *RGH1* candidacy for *Rmo1* resistance, we took advantage of an introgression panel containing diverse mildew resistance loci. The Siri near-isogenic lines (NILs) contain 13 mildew resistance genes, including 11 *Mla* specificities, in isogenic background of Siri including *Mla1*, *Mla3*, *Mla6*, *Mla7* (Nordal), *Mla7* (Moseman), *Mla9*, *Mla10*, *Mla12*, *Mla13*, *Mla22*, *Mla23*, *Ml-(Ru2)*, and *Mlk* (Kølster and Stølen 1987). Inoculation of the Siri NILs with *M. oryzae* isolate KEN54-20 using a spray- and spot-based inoculation found that line S02 containing *Mla3* and the line S13 carrying *Mla23* were resistant to KEN54-20 (Fig. 4; Supplemental Fig. S4). *Mla23* is the most closely related *Mla* allele to *Mla3*, sharing 98% sequence similarity at the DNA and protein level, with variation limited to the C-terminal region of the LRR (Supplemental Fig. S5) (Seeholzer et al. 2010). Leaf RNA-seq data of S13 confirmed the expression of *Mla23* but did not detect *RGH2* or *RGH3*. The close phylogenetic relationship between *Mla3* and *Mla23* supports the hypothesis that *Mla3* underlies *Rmo1*-mediated resistance.

To confirm *Rmo1*, all 4 candidate genes were cloned via PCR amplification—*Mla3* and *Mla3Δ6* from cDNA and *RGH2* and *RGH3* from gDNA. *Mla3* and *Mla3Δ6* were placed in an expression construct containing the *Mla6* promoter and terminator (Supplemental Fig. S6). The *Mla6*

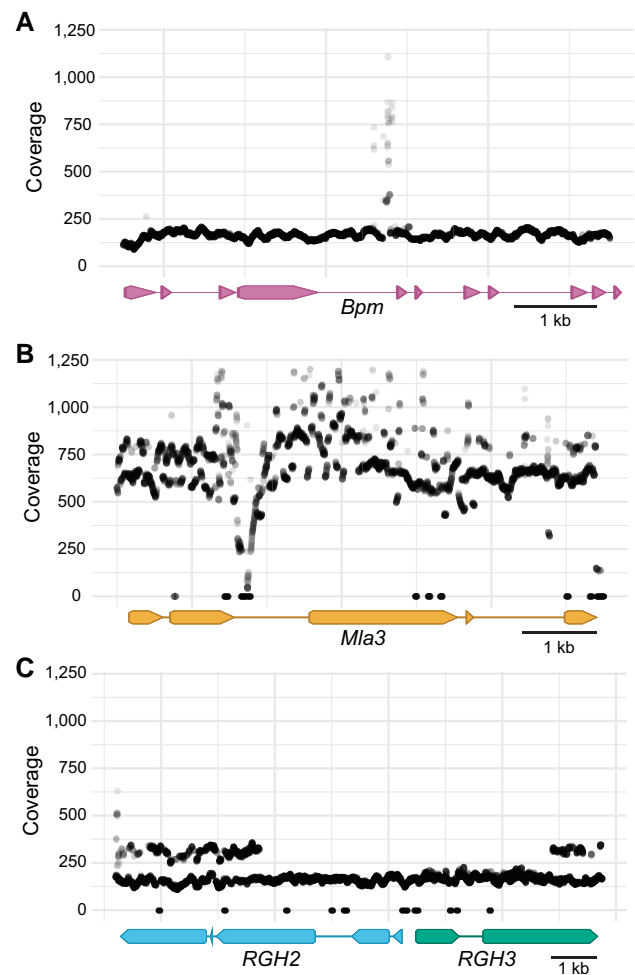


**Figure 3.** *k*-mer analysis identifies 4 copies of *Mla3* in barley accession Baronesse. **A)** *k*-mer coverage of *Bpm*. *Bpm* is located proximal to the *Mla* locus and exists as a single copy with coverage centered at 175. **B)** *k*-mer coverage of *Mla3*. Two coverage bands are observed at 619 and 790 coverage, corresponding to 4 and 5 copies. Reduced coverage in the second intron is due to the presence of low complexity sequence (dinucleotide repeat). **C)** *k*-mer coverage of *RGH2* and *RGH3*. Two coverage bands are observed at 162 and 315 coverage, corresponding to 1 and 2 copies, respectively. The additional copies represent fragments of *RGH2* and *RGH3*, which are located in the distal and proximal boundaries of the *Mla* locus (Fig. 2A). Zero *k*-mer coverage represents inaccurate sequence calls from RenSeq-PacBio sequencing in contigs encompassing *Mla3* and *RGH2/3*. Gene models are shown below each plot with exons and introns shown as arrows and lines, respectively.

promoter/terminator system was selected for direct comparison of *Mla3* and *Mla3Δ6* by eliminating native promoter variation. *RGH2* and *RGH3* were maintained in the native form and head-to-head orientation (Supplemental Fig. S6). All constructs were transformed into the barley accession Golden Promise as Golden Promise is susceptible to *Bgh* isolate CC148 (*AVR<sub>a3</sub>*) and *M. oryzae* isolate KEN54-20 (*AVR-Rmo1*). *Mla3*, *Mla3Δ6*, and *RGH2/3* transgenic Golden Promise T<sub>1</sub> families were tested with the *Bgh* isolate CC148 (*AVR<sub>a1</sub>*, *AVR<sub>a3</sub>*, and *avr<sub>a6</sub>*). Eight seeds from 2 spikes

Accession	Allele			<i>B. graminis</i> f. sp. <i>hordei</i> CC148	<i>M. oryzae</i> KEN54-20
	RGH1	RGH2	RGH3		
Baronesse	<i>Mla3</i>	<i>RGH2.a</i>	<i>RGH3.a</i>		
Siri	<i>Mla8</i>	ND	ND		
S02	<i>Mla3</i>	<i>RGH2.a</i>	<i>RGH3.a</i>		
S13	<i>Mla23</i>	ND	ND		
Maritime	<i>RGH1.Mar</i>	<i>RGH2.a</i>	<i>RGH3.a</i>		

**Figure 4.** Coupling of *Mla3* and *Rmo1* in diverse barley accessions. Disease phenotypes of barley accessions carrying different alleles of the candidate genes *RGH1*, *RGH2*, and *RGH3* inoculated with *Bgh* isolate CC148 and *M. oryzae* isolate KEN54-20. The haplotypes of the barley accessions are listed on the left-hand side with the allele of *RGH1*, *RGH2*, and *RGH3* indicated. ND, gene was not detected in RNA-seq data.

were evaluated per family. Four independent  $T_1$  families were evaluated for *Mla3* ( $T_{1-3}$ ,  $T_{1-4}$ ,  $T_{1-5}$ , and  $T_{1-6}$ ); 4  $T_1$  families were evaluated for *Mla3Δ6* ( $T_{1-2}$ ,  $T_{1-3}$ ,  $T_{1-6}$ , and  $T_{1-7}$ ); and 7  $T_1$  families for *RGH2/RGH3* ( $T_{1-1}$ ,  $T_{1-3}$ ,  $T_{1-4}$ ,  $T_{1-5}$ ,  $T_{1-9}$ ,  $T_{1-11}$ , and  $T_{1-12}$ ). Only full-length *Mla3* was shown to confer resistance to *Bgh* isolate CC148, with transgenic *Mla3Δ6* lines displaying susceptibility (Fig. 5). *Mla3Δ6* is 98% identical in coding and protein sequence to *Mla3*. *Mla3Δ6* could represent a loss-of-function allele or pseudogene of *Mla3*. All *RGH2/RGH3* transgenic barley  $T_1$  families were susceptible to *Bgh* isolate CC148 (Fig. 5A).

*Rmo1* confers dominant, race-specific resistance to *M. oryzae* isolate KEN54-20 (*AVR-Rmo1*) (Inukai et al. 2006). *Mla3*, *Mla3Δ6*, and *RGH2/RGH3* transgenic  $T_1$  families were screened with *M. oryzae* isolate KEN54-20 using spot inoculation on detached leaves. Eight seeds from 2 spikes were evaluated per family. Four independent  $T_1$  families were evaluated for *Mla3* ( $T_{1-3}$ ,  $T_{1-4}$ ,  $T_{1-5}$ , and  $T_{1-6}$ ); 4  $T_1$  families were evaluated for *Mla3Δ6* ( $T_{1-2}$ ,  $T_{1-3}$ ,  $T_{1-6}$ , and  $T_{1-7}$ ); and 7  $T_1$  families for *RGH2/RGH3* ( $T_{1-1}$ ,  $T_{1-3}$ ,  $T_{1-4}$ ,  $T_{1-5}$ ,  $T_{1-9}$ ,  $T_{1-11}$ , and  $T_{1-12}$ ). *Mla3* transgenic lines showed resistance to *M. oryzae* KEN54-20 (Fig. 5A; Supplemental Data Set 2). Analysis of segregating *Mla3* transgenic  $T_1$  families showed phenotypic variation, with some families displaying partial or no resistance. In contrast, *Mla3Δ6* transgenic lines were susceptible to KEN54-20. All *RGH2/RGH3* transgenic individuals were fully susceptible. Collectively, resistance to both *Bgh* and *M. oryzae* was only observed in transgenic families carrying *Mla3*, although substantial intrafamily variation was observed for *M. oryzae*.

### Multiple copies of *Mla3* are required for *M. oryzae* resistance

Based on the observation of variable expression in *Mla3*  $T_1$  families for resistance to *M. oryzae* KEN54-20, we hypothesized that sufficient expression of *Mla3* is required to confer resistance. Natively, copy number variation is observed in wild-type Baronesse with 3 copies of *Mla3* and 1 copy of

*Mla3Δ6* in the haploid genome. Therefore, we evaluated copy number variation of the individual transgenic lines. For the *Mla3*  $T_1$  families ( $T_{1-1}$ ,  $T_{1-4}$ ,  $T_{1-5}$ , and  $T_{1-6}$ ), the number of copies ranged from 0 to 6. For the *Mla3Δ6*  $T_1$  lines, the number of copies of the transgenic insert varied from 1 to 4. Copy number analysis of the *RGH2/RGH3*  $T_1$  lines varied from 0 to 4 copies. Evaluation of copy number variation in  $T_1$  families and their phenotypic response to *M. oryzae* isolate KEN54-20 found an inverse linear correlation (Fig. 5B). Multiple copies of *Mla3* were required to complement the wild-type phenotype and confer complete resistance to *M. oryzae* isolate KEN54-20 (Fig. 5B). Resistance was only observed in individuals carrying greater than 2 copies of the insert, with a single copy being insufficient for complementation (Fig. 5B).

Due to the high copy number being required for complementation in the transgenic lines, it was unclear if the observed resistance could be due to autoactivity of the transgene. Overexpression of NLRs has been shown to cause constitutive defense activation and broad-spectrum disease resistance to multiple pathogens (Lai and Eulgem 2018; Li et al. 2019). To evaluate this, resistant *Mla3* transgenic lines were tested with *M. oryzae* isolate Sasa2 (*avr-Rmo1*), which is virulent on wild-type Baronesse carrying *Mla3*. Transgenic *Mla3* lines with high copy number that previously displayed resistance to *M. oryzae* isolate KEN54-20 were spot inoculated with *M. oryzae* isolates KEN54-20 and Sasa2 in single spots in proximal and distal positions on detached leaves (Fig. 6). *Mla3* shows specific recognition of *M. oryzae* isolate KEN54-20 similar to wild-type Baronesse but was susceptible to *M. oryzae* isolate Sasa2, showing large susceptible lesions (Fig. 6). The barley accessions Golden Promise and Nigrata are susceptible to *M. oryzae* isolates KEN54-20 and Sasa2. Resistance to *M. oryzae* isolate KEN54-20 was maintained regardless of spot inoculation position on the leaf. Thus, *Mla3* provides isolate-specific resistance

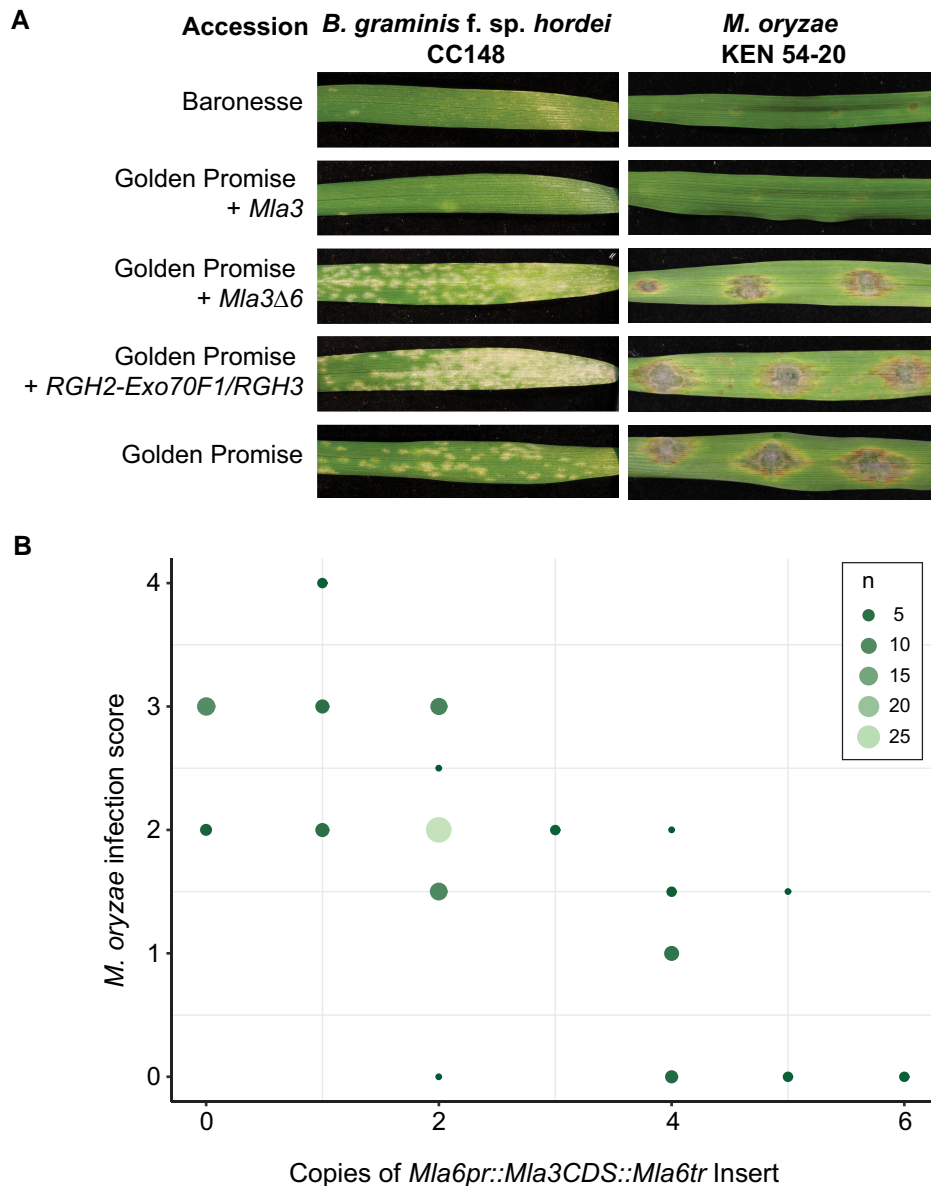


**Figure 5.** *Mla3* confers resistance to *Bgh* isolate CC148 and *M. oryzae* isolate KEN54-20. **A)** Transgenic lines of *Mla3* (T<sub>1</sub>-4), *Mla3Δ6* (T<sub>1</sub>-7), and *RGH2/RGH3* (T<sub>1</sub>-9) inoculated with *Bgh* isolate CC148 carrying AVR<sub>a3</sub> and transgenic lines of *Mla3* (T<sub>1</sub>-4), *Mla3Δ6* (T<sub>1</sub>-3 T<sub>2</sub>), and *RGH2/RGH3* (T<sub>1</sub>-5) *M. oryzae* isolate KEN54-20. Controls include resistant wild-type Baronesse and susceptible wild-type Golden Promise used for transformation. Complete resistance shown to *Bgh* and *M. oryzae* by Baronesse and transgenic line Golden Promise + *Mla3*, whereas wild-type Golden Promise and transgenic lines Golden Promise + *Mla3Δ6* and +*RGH2/RGH3* are susceptible. Phenotypes are representative of inoculated T<sub>1</sub> families. **B)** Two independent T<sub>1</sub> families of Golden Promise + *Mla3* (T<sub>1</sub>-4 and T<sub>1</sub>-5) showing resistance with varying copy numbers (0 to 6) inoculated with *M. oryzae* isolate KEN54-20. Phenotypic scores 0 and 1 = resistant and 2 to 4 = susceptible. The plot shows the total number of individual lines from merged T<sub>1</sub> families with insert copy number and phenotypic scores based on circle size. The smallest circles ≤5 individuals to large circles = 25 individuals).

to KEN54-20 hypothesized through recognition of the effector AVR-*Rmo1* present in KEN54-20 but not Sasa2.

#### AVR-*Rmo1* is Pwl2

To identify the effector AVR-*Rmo1* that is recognized by *Mla3*, we performed mutagenesis on spores of *M. oryzae* isolate KEN54-20 through exposure to UV light and screened for gain-of-virulence mutants on wild-type Baronesse following

spray-based inoculation. Gain of virulence (*avr-rmo1*) was confirmed in 12 mutants following reinoculation on Baronesse using a spot-based method on both wild-type Baronesse (*Mla3*) and *Mla3* transgenic lines (T<sub>1</sub>-4 T<sub>2</sub>) (Supplemental Fig. S7). To identify AVR-*Rmo1*, we first sequenced the genome of *M. oryzae* isolate KEN54-20. To identify shared mutations in the mutants, we performed whole genome sequencing of the mutants and compared to the



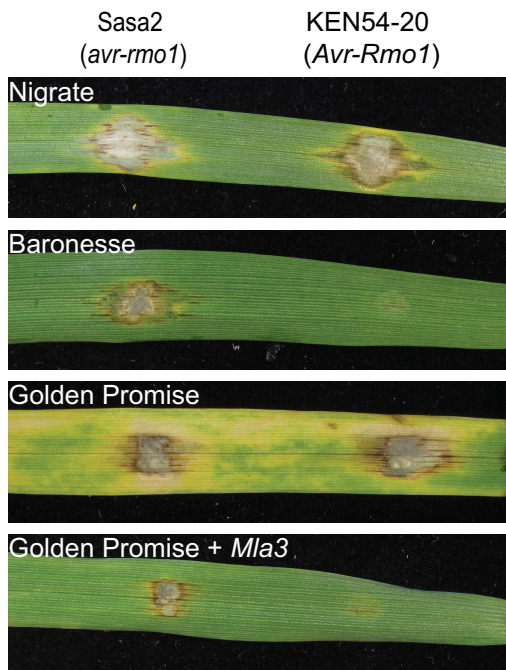


**Figure 6.** *Mla3* confers isolate-specific resistance to *M. oryzae*. Transgenic Golden Promise + *Mla3* (T<sub>1</sub>-4 T<sub>2</sub>) spot inoculated with *M. oryzae* isolates KEN54-20 (*AVR-Rmo1*) and Sasa2 (*avr-Rmo1*). *Mla3* confers resistance to isolates carrying *AVR-Rmo1*. Controls Golden Promise and hypersusceptible Nigrate are susceptible to both Sasa2 and KEN54-20.

wild-type KEN54-20 genome. A window-based *k*-mer analysis was used to identify regions harboring SNPs, insertions, or deletions in all mutant lines. A region of 8 kb encompassing the known effector *PWL2* was deleted across all mutant lines (Supplemental Fig. S8) (Sweigard et al. 1995). The exact boundaries of the deletions in each mutant are ambiguous due to repetitive regions in the flanking sequence of *PWL2*, but manual inspection of aligned reads to the region confirmed the deletion of the *PWL2* coding sequence in each mutant line. However, gain of virulence to *Mla3* could also be due to other independent mutations in each mutant line or loss of a closely linked gene in the shared *PWL2* deletion.

To determine whether *PWL2* is *AVR-Rmo1*, we complemented mutant *M. oryzae* lines with *PWL2* expressed under its native promoter. Independent ectopic transformed mutant lines of *M. oryzae* (M43 + *pPWL2:PWL2* transformant 4 and M61 + *pPWL2:PWL2* transformant 1) were avirulent on Baronesse (*Mla3*) and transgenic *Mla3* plants (Fig. 7) confirming that *PWL2* is *AVR-Rmo1*.

### MLA3 recognizes Pwl2 in transient expression assays in *Nicotiana benthamiana*

Previous work has established that transient expression of MLA alleles recognizing *Bgh* AVR<sub>a</sub> effectors in *Nicotiana benthamiana* elicits an effector-dependent hypersensitive response (Saur et al. 2019; Bauer et al. 2021). To assess whether MLA3 specifically triggers cell death upon recognition of

Pwl2, we transiently coexpressed MLA3 with Pwl2 or AVR<sub>a10</sub> in this heterologous system. We found that MLA3 responds to Pwl2 (observed as strong cell death) but not to AVR<sub>a10</sub> (Fig. 7C). Cell death was elicited without coexpression of additional components in *N. benthamiana*. Pwl2 and AVR<sub>a10</sub> alone did not trigger hypersensitive response. These results indicate that MLA3 specifically recognizes Pwl2.

### MLA3 and Pwl2 associate in planta

To investigate whether Pwl2 recognition by MLA3 correlates with association between the 2 proteins, we tested the ability of MLA3 to coimmunoprecipitate with Pwl2 in plant protein extracts. Due to the strong cell death response elicited upon Pwl2 recognition by MLA3 in *N. benthamiana*, we introduced the L11E mutation in the very N-terminal  $\alpha$ 1-helix of MLA3 (MLA3<sup>L11E</sup>) to facilitate biochemical studies. Mutations in this region of other CC-NLRs with a MADA motif or a MADA-like motif, like MLA, dampen or abolish cell death induction without compromising potential effector association and/or resistosome formation (Adachi et al. 2019; Ahn et al. 2023; Contreras et al. 2023). As expected, MLA3<sup>L11E</sup> does not elicit a strong hypersensitive response upon recognition of Pwl2, in contrast to wild-type MLA3 (Supplemental Fig. S9). To assess the ability of MLA3<sup>L11E</sup> to associate with Pwl2 in planta, we transiently coexpressed Pwl2 C-terminally fused to a 3x-FLAG tag (Pwl2-FLAG) and MLA3<sup>L11E</sup> C-terminally tagged with a 6xHA epitope (MLA3<sup>L11E</sup>-HA) for 72 h. Protein extracts were incubated with  $\alpha$ -HA or  $\alpha$ -FLAG affinity beads to immunoprecipitate the corresponding tagged proteins. Immunoprecipitation of MLA3<sup>L11E</sup> pulled down Pwl2 but not AVR<sub>a10</sub>, which was used as negative control (Fig. 7D).

To test the ability of other MLA alleles to associate with Pwl2, we introduced the L11E mutation in the MLA10 allele (MLA10<sup>L11E</sup>) to abolish its autoactivity (Supplemental Fig. S9) and transiently coexpressed it with AVR<sub>a10</sub> and Pwl2. Surprisingly, AVR<sub>a10</sub> did not coimmunoprecipitate with MLA10<sup>L11E</sup> (Fig. 7D) despite previous results of direct effector recognition by MLA10 (Saur et al. 2019). This could likely be explained by a fast, transient protein–protein interaction in planta. In addition, Pwl2 was not pulled down by immunoprecipitation of MLA10<sup>L11E</sup> (Fig. 7D). Similar results were observed when  $\alpha$ -FLAG affinity beads were used to pull down Pwl2 or AVR<sub>a10</sub> (Fig. 7E). Only MLA3<sup>L11E</sup>, but not MLA10<sup>L11E</sup>, was detected after immunoprecipitation of Pwl2, and none of the tested MLA alleles were detected after pulling down AVR<sub>a10</sub> (Fig. 7E). This is the first report of an MLA allele immunoprecipitating with its cognate effector in planta, as it has not been shown for other MLA-AVR<sub>a</sub> corresponding pairs. The strong association between MLA3 and Pwl2 in *N. benthamiana* indicates that recognition of Pwl2 occurs upon specific interaction with MLA3.

### Conserved recognition specificity of *PWL2* in barley and weeping lovegrass

*PWL2* conditions the ability of rice-infecting *M. oryzae* isolates to infect weeping lovegrass (*Eragrostis curvula*) and is

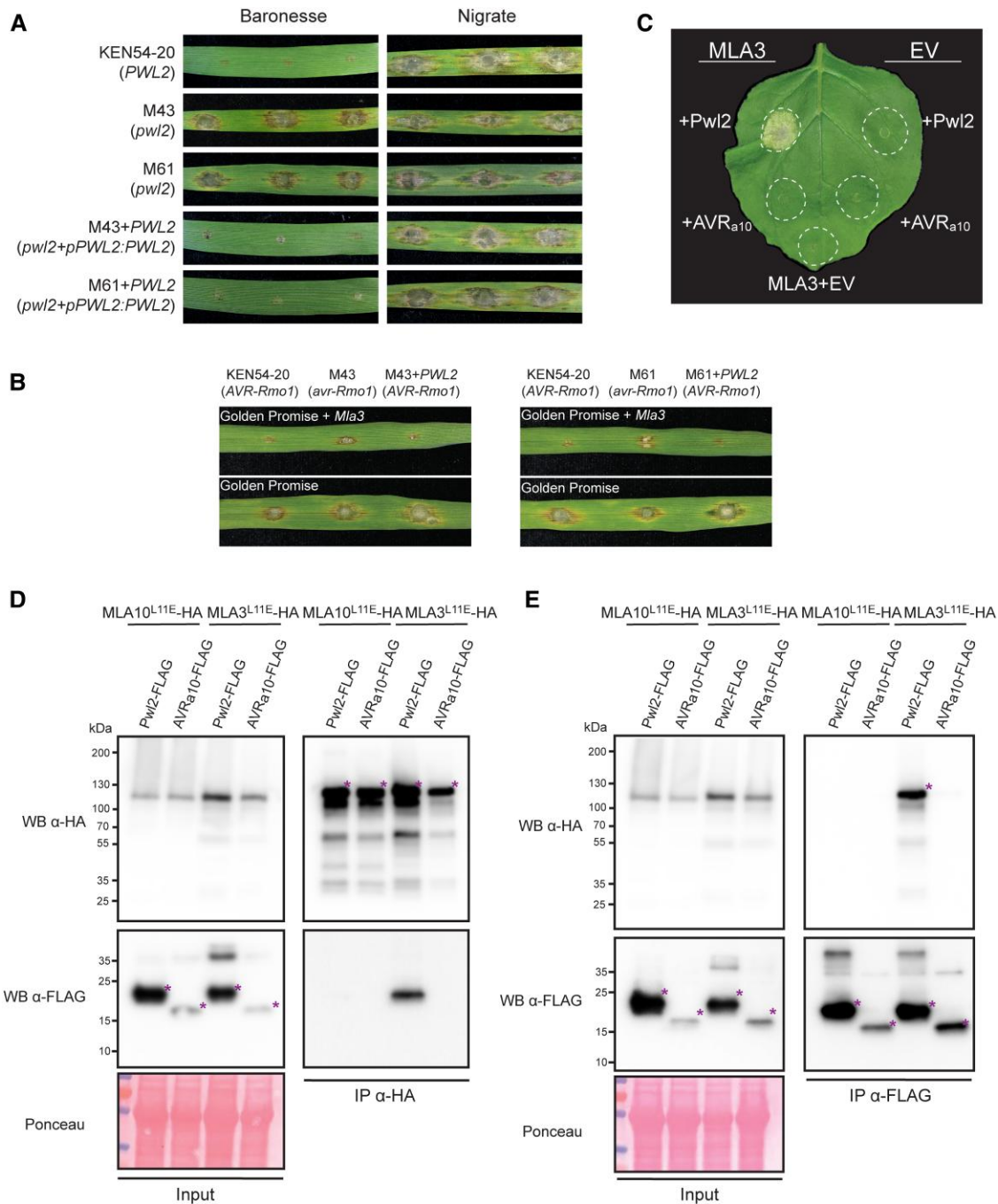


**Figure 7.** MLA3 recognizes and interacts with Pwl2. **A**) *PWL2* complements *M. oryzae avr-Rmo1* mutants. Baronesse (*Mla3*) leaves spot inoculated with *M. oryzae* KEN54-20 (*AVR-Rmo1*) and *avr-Rmo1* mutants M43 and M61. *M. oryzae* isolate KEN54-20 is avirulent on Baronesse, whereas *avr-Rmo1* mutants M43 and M61 are virulent. Ectopic integration of *PWL2* driven by native promoter (*pPWL2:PWL2*) complements the phenotype of mutants M43 and M61. Susceptible control, Nigratte. **B**) *Mla3* recognizes *PWL2* in transgenic Golden Promise + *Mla3*. Transgenic Golden Promise + *Mla3* ( $T_1$ - $T_2$ ) spot inoculated with *M. oryzae* isolate KEN54-20 (*AVR-Rmo1*), *avr-Rmo1* mutants M43 and M61, and *avr-Rmo1* mutants M43 and M61 transformed with *PWL2* driven by its native promoter (*pPWL2:PWL2*). Susceptible control, Golden Promise. **C**) Transient expression of MLA3 with Pwl2 in *N. benthamiana* triggers hypersensitive response. Representative *N. benthamiana* leaf infiltrated with *A. tumefaciens* strains carrying the corresponding binary expression constructs. AVR<sub>a10</sub> and empty vector (EV) were used as negative controls. Leaves were photographed 3 d after agroinfiltration. The experiment was independently repeated 3 times with 6 to 9 technical replicates. **D, E**) MLA3 interacts with Pwl2 in planta. Coimmunoprecipitation experiment of C-terminally 6xHA-tagged MLA3<sup>L11E</sup> and MLA10<sup>L11E</sup> with C-terminally 3xFLAG-tagged Pwl2 and AVR<sub>a10</sub>. Proteins obtained by coimmunoprecipitation with α-HA beads **D**) or α-FLAG beads **E**) and total protein extracts (input) were separated by SDS-PAGE and detected by immunoblotting using the appropriate antibodies labeled on the left of each blot. Asterisks indicate protein bands of the corresponding expected size. The experiments were independently performed 3 times with similar results.

a major determinant of host–species specificity (Kang et al. 1995; Sweigard et al. 1995). To confirm loss of *PWL2* function, we tested whether KEN54-20 mutants M43 and M61 were virulent on weeping lovegrass due to loss of *PWL2*. Weeping lovegrass was resistant to spray inoculation of wild-type KEN54-20, yet infection of 2 independent mutant lines resulted in susceptible lesions and restriction of plant growth (Fig. 8). Ectopic transformation of *PWL2* in the independent mutants (M43 + *pPWL2:PWL2* and M61 + *pPWL2:PWL2*) made them avirulent on *E. curvula* (Fig. 8A). *PWL2* is part of the *PWL* multigene family and is highly prevalent across isolates (Valent et al. 1986; Kang et al. 1995; Sweigard et al. 1995). *pwl2-2* encodes an allele of *PWL2* that contains a single nonsynonymous (D90N) substitution resulting in the loss of recognition and subsequent virulence on weeping lovegrass (Kang et al. 1995; Sweigard et al. 1995; Schneider et al. 2010).

To test whether the same nonsynonymous mutation would abolish recognition by *Mla3*, diverse *M. oryzae* isolates

were inoculated on Baronesse (Fig. 8B). Five *M. oryzae* isolates carrying wild-type *PWL2* were avirulent on Baronesse (*Mla3*) (Fig. 8B). The *M. oryzae* isolate Ina168, known to lack *PWL2*, was virulent on Baronesse. In agreement with the previous reports on weeping lovegrass (Sweigard et al. 1995), *M. oryzae* isolates carrying the *pwl2-2* allele (*PWL2* D90N) were not recognized by *Mla3* and therefore virulent on Baronesse. The isolates Naga69-150, Ina85-182, and Ina87T-156A, which carry both *PWL2* and *pwl2-2*, were avirulent on Baronesse due to recognition of the wild-type *PWL2*. These results provide evidence that recognition of *PWL2* is conserved in barley and weeping lovegrass, and specificity of recognition is maintained in both grass species.

### Weeping lovegrass lacks an *Mla* ortholog

The resistance gene in weeping lovegrass that recognizes *PWL2* is unknown. To determine whether an *Mla* ortholog is present in weeping lovegrass and related grass species,

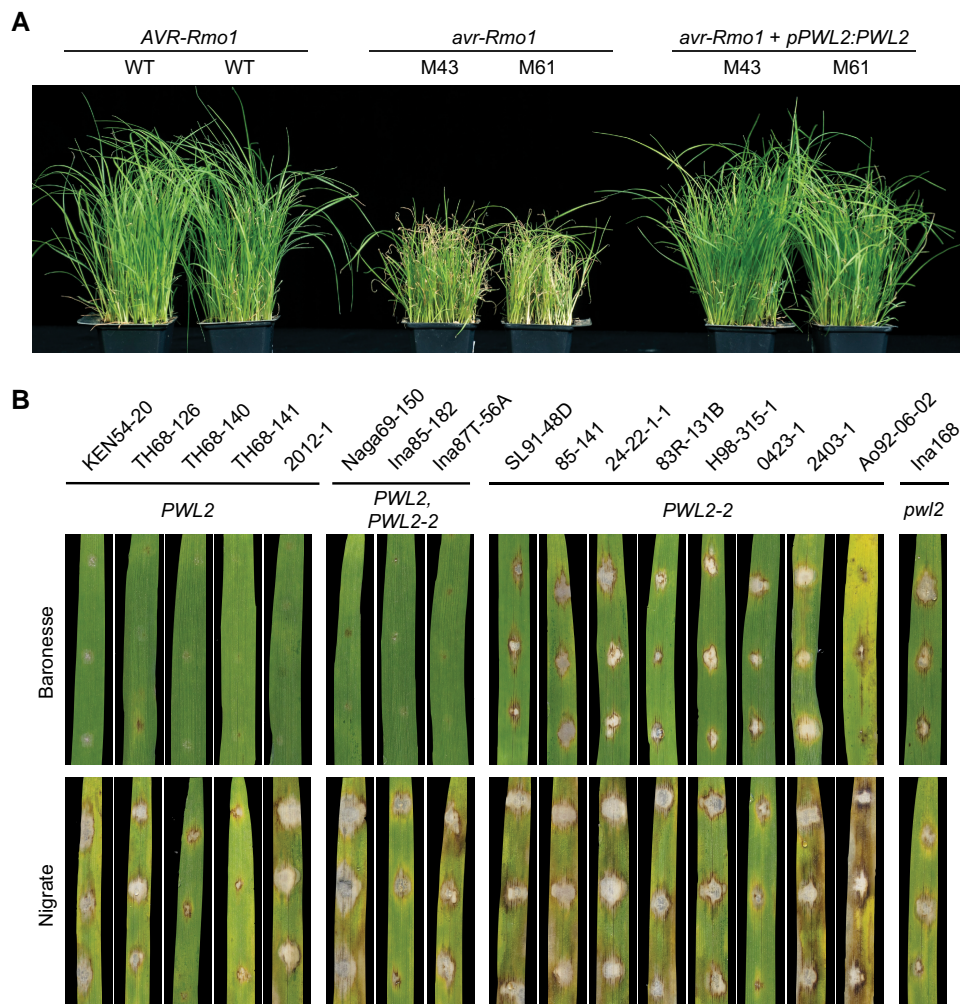


**Figure 8.** Conserved recognition specificity of *PWL2* in barley and weeping lovegrass. **A**) Weeping lovegrass spray infected with *M. oryzae* isolates with and without *AVR-Rmo1* (*PWL2*). WT: *M. oryzae* isolate KEN54-20 (*AVR-Rmo1*), *avr-Rmo1* (*pwl2*) mutants M43 and M61, and *avr-Rmo1* (*pwl2*) mutants M43 and M61 transformed with *PWL2* driven by its native promoter (*pPWL2:PWL2*). **B**) Baronesse (*Mla3*) spot inoculated with 17 *M. oryzae* isolates representing *PWL2* natural variation. The isolates Naga69-150, Ina85-182, and Ina87T-56A carry both *PWL2* and *pwl2-2*. Susceptible control, Nigrate. Phenotypes are representative of 3 biological replicates with 3 technical replicates.

we constructed a maximum likelihood phylogenetic tree using protein sequence for NB domains from NLRs of 7 grass species: barley (*H. vulgare*) (Mascher et al. 2021), weeping lovegrass (*E. curvula*) (Carballo et al. 2019), *Brachypodium distachyon* (Vogel et al. 2010), rice (*O. sativa*) (Goff et al. 2002), maize (*Zea mays*) (Schnable et al. 2009), *Setaria italica* (Bennetzen et al. 2012), and *Sorghum bicolor* (Paterson et al. 2009). These species have high-quality genomes and annotations and are balanced in representation between PACMAD and BOP clades. Superposition of previous clade classifications found that the *RGH1* (*Mla*) gene family is in the C17 clade (Supplemental Fig. S10) (Bailey et al. 2018). Phylogenetic analysis of the C17 clade found 34 NLRs from *B. distachyon*, 36 NLRs from barley, 36 NLRs from rice, 30 NLRs from *S. bicolor*, 49 NLRs from *S. italica*, 25 NLRs from *Z. mays*, and 101 NLRs from weeping lovegrass in the C17 clade. While bootstrap support exists for many subclades that found orthologous NLRs from the majority of grasses, the subclade including *RGH1* only had members from barley and *B. distachyon* (Supplemental Fig. S11). Thus, the *RGH1* family and related NLRs are predominantly absent in the evaluated sequenced species from the PACMAD clade, in which weeping lovegrass resides. Therefore, recognition of *PWL2* in *E. curvula* is likely conferred by a resistance gene outside of the *RGH1* family.

## Discussion

The majority of NLRs confer resistance in a pathogen species- or isolate-specific manner. *Mla* alleles have been well studied for isolate-specific resistance to *Bgh* through the functional divergence of alleles (Jørgensen and Wolfe 1994; Seeholzer et al. 2010; Saur et al. 2019). However, while resistance to multiple pathogens has been mapped to the *Mla* locus across barley haplotypes, many of the underlying causal genes have yet to be identified due to the limitations of suppressed recombination across the locus and the inability to assemble the region with current genomic tools. Homologs of *Mla*, *Sr33* in wheat (*Triticum aestivum*) and *Sr50* in rye (*Secale cereale*), confer disease resistance to diverse races of stem rust pathogen *Puccinia graminis* f. sp. *tritici*, including the virulent isolate TTKSK (Periyannan et al. 2013; Chen et al. 2017). *Mla*, *Sr33*, and *Sr50* highlight the potential for orthologous genes to evolve new and different pathogen specificities, expanding the breadth of recognition of the *Mla* gene family across a diversity of ascomycete and basidiomycete pathogens. In comparison, *Mla8* (= *Rps7*) was shown to confer resistance to both *Bgh* and *P. striiformis* f. sp. *tritici* (Bettgenhaeuser et al. 2021). Here, we confirm that the barley NLR *MLA3* recognizes the effector *Pwl2* from *M. oryzae* and show that this single NLR is capable of recognition of 2 taxonomically diverse pathogens. *MLA3* specifically recognizes the host-specificity determinant *Pwl2*, as loss of this effector permits successful infection by *M. oryzae* and transient coexpression of *MLA3* and *Pwl2* in *N. benthamiana* triggers a strong hypersensitive response. Therefore, *Mla3* has evolved the capacity to

recognize host-adapted effectors from *Bgh* and convergently recognizes an important host-determining effector from *M. oryzae*, further expanding the multiple pathogen recognition of the *Mla* locus.

As a species, *M. oryzae* is known to infect a wide range of cultivated and wild grass plant species; however, individual isolates have a narrow host range due to incompatibility factors present in the plant (Ou 1985; Couch and Kohn 2002; Gladieux et al. 2018; Jacob 2021). Recently, the emergence of the wheat infecting lineage of the blast fungus, the *M. oryzae* *Triticum* pathotype, was found to be due to the sequential loss of specific effectors encoded by *PWT3* and *PWT4* (Inoue et al. 2017). The corresponding wheat R genes *Rwt3* and *Rwt4* were responsible for incompatibility of *M. oryzae* during infection, and their separation facilitated *M. oryzae* step-wise adaptation to become a pathogen of wheat (Inoue et al. 2017). Members of the *Pathogenicity toward Weeping Lovegrass* (*PWL*) multigene family—*PWL1*, *PWL2*, *PWL3*, and *PWL4*—contribute to host specialization of *M. oryzae* pathotypes (Valent et al. 1986; Kang et al. 1995; Sweigard et al. 1995). *PWL1*, first identified from finger millet (*Eleusine coracana*) isolates, and *PWL2*, first identified in rice isolates, prevent infection on weeping lovegrass (*E. curvula*) and therefore condition host-specificity (Kang et al. 1995; Sweigard et al. 1995; Masaki et al. 2023). Small amino acid changes in the *Pwl2* effector are sufficient to abolish recognition and allow virulence (Schneider et al. 2010), yet *PWL2* displays low genetic variation within populations across geographic locations and the majority of isolates pathogenic on rice contain *PWL2* (Sweigard et al. 1995; Huang et al. 2014; Sirisathaworn et al. 2017). Widespread prevalence of *PWL2* in rice-infecting lineages would be facilitated by lack of resistance genes to *PWL2* in rice. As yet, the resistance gene in weeping lovegrass that recognizes *PWL2* has not been identified, and the mechanism underlying recognition in this grass species remains unknown. The lack of a clear *Mla* ortholog in weeping lovegrass, the specific recognition of *Pwl2* by *MLA3*, and the conserved specificity of *Pwl2* recognition strongly suggest that *MLA3* and an unknown resistance gene in weeping lovegrass convergently evolved toward *Pwl2* recognition.

Individual NLRs often have a narrow specificity due to their recognition of a single effector. At a population level, an allelic series of NLRs may collectively have broader recognition through perception of diverse effectors (Dangl and Jones 2001; Brown and Tellier 2011). The allelic flax rust (*Melampsora lini*) resistance gene *L* was the first to be described (Flor 1956), and the additional *K*, *M*, *N*, and *P* loci encode further closely linked or allelic genes (Ravensdale et al. 2011). The *A. thaliana* *RECOGNITION OF PERONOSPORA PARASITICA 8* (*RPP8*) gene family encodes NLRs with diverse resistance specificities, with alleles conferring resistance to the oomycete *Hyaloperonospora arabidopsidis* (*RPP8*), *Turnip crinkle virus* (*HRT*), and *Cucumber mosaic virus* (*RCY1*) (McDowell et al. 1998; Cooley et al. 2000; Takahashi et al. 2002; Kuang et al. 2008). It is hypothesized that unequal crossovers that generate chimeras between alleles are a

driving force for new *RPP8* specificities (McDowell et al. 1998; Ding et al. 2007). Similar to the *Mla* alleles of barley recognizing *Bgh*, the wheat *Powdery mildew 3 (Pm3)* alleles recognize *B. graminis* f. sp. *tritici* (wheat powdery mildew) *AvrPm3* effectors which are sequence unrelated but structurally similar (Bourras et al. 2018, 2019). Direct NLR–effector interaction can drive coevolution and diversification of NLR and effector repertoires, through opposing selection on NLRs to maintain effector recognition and selection on effectors to avoid triggering resistance (Van der Hoorn et al. 2002; Saur et al. 2021). However, changes to effector structure to avoid recognition may be constrained by effector function. For example, many bacterial pathogen species contain the effector *AvrRpt2* which is important for virulence, and recognition of *AvrRpt2* is conserved across plant species (Mazo-Molina et al. 2020). There may be a limitation on the functional and structural variation of effectors that are vital for pathogenesis.

Direct recognition has been described for *Bgh* effectors *AVR<sub>a1</sub>*, *AVR<sub>a7</sub>*, *AVR<sub>a10</sub>*, *AVR<sub>a13</sub>*, and *AVR<sub>a22</sub>* and the *Mla* alleles *MLA1*, *MLA7*, *MLA10*, *MLA13*, and *MLA22*, respectively (Lu et al. 2016; Saur et al. 2019). Recognition is highly specific as only the interaction of the *Mla* allele with the matching *Bgh* *AVR<sub>a</sub>* activates cell death in barley protoplasts and heterologous systems (Chen et al. 2017; Saur et al. 2019). Recognition specificity is largely determined by the MLA LRR domain and few residues located in different surfaces in the AVR proteins (Shen et al. 2003; Halterman and Wise 2004; Seeholzer et al. 2010; Bauer et al. 2021; Cao et al. 2023). Known *Bgh* *AVR<sub>a</sub>* effectors are sequence unrelated (apart from the allelic *AVR<sub>a10</sub>* and *AVR<sub>a22</sub>*) and share a conserved structural fold (Saur et al. 2019; Bauer et al. 2021; Cao et al. 2023). *AVR<sub>a6</sub>* belongs to the family of catalytically inactive RNase-Like Proteins expressed in Haustoria (RALPHs), and similar RNase-like folds are present in *AVR<sub>a1</sub>*, *AVR<sub>a7</sub>*, *AVR<sub>a10</sub>*, *AVR<sub>a13</sub>*, and *AVR<sub>a22</sub>* (Cao et al. 2023). A common structural scaffold shared by the RALPH effector family may therefore be driving diversification of MLA alleles (Bauer et al. 2021). In comparison, the *P. graminis* f. sp. *tritici* effector *AVR-Sr50* directly binds the MLA homolog *SR50*, and its structure does not resemble known *Bgh* AVRs (Chen et al. 2017; Ortiz et al. 2022). For *Mla3*, *AVR<sub>a3</sub>* has not yet been identified. AlphaFold2 structure prediction of *PWL2* (Jumper et al. 2021) and subsequent structural comparisons on the Dali server (Holm 2022) show that *PWL2* does not contain an RNase-like fold and belongs to the group of MAX effectors (*M. oryzae* *Avrs* and *ToxB*), which is an expanded family of sequence unrelated but structurally similar effectors in *M. oryzae* (de Guillen et al. 2015). In addition, structural prediction studies indicate that the MAX effector family is absent from the *Bgh* effector repertoire (Seong and Krasileva 2022).

Here we show that *Pwl2* recognition is triggered upon specific association with *MLA3* in *N. benthamiana*. This interaction was sufficiently strong and stable to be detected in coimmunoprecipitation assays, which has not been shown

before for other *MLA-AVR<sub>a</sub>* corresponding pairs. Even though different *MLA* alleles directly recognize *Bgh* *AVR<sub>a</sub>* effectors, these protein–protein interactions may be transient and therefore nondetectable by protein pull-down experiments. However, the interaction between *MLA3* and *Pwl2* was clear and robust in the *N. benthamiana* heterologous system. Considering the evidence supporting direct recognition of *Bgh* *AVR<sub>a</sub>* effectors by different *MLA* alleles, the evolutionary trajectory of *Mla*, and the phylogenetic distance between *N. benthamiana* and barley, direct recognition of *Pwl2* by *MLA3* remains the most parsimonious model of recognition. The question of how sequence similar *Mla* alleles recognize structurally distinct effectors from diverse pathogen species remains. Documented cases of multiple pathogen recognition by NLRs are rare, and all instances studied to date involve sensing of conserved effector activities on shared host targets that act as guardees or decoys or on integrated domains of NLRs (Lewis et al. 2013; Sarris et al. 2015; Wang et al. 2015; Zhang et al. 2017; Mukhi et al. 2021). The TIR-NLR *ROQ1* directly recognizes the effectors *HopQ1*, *XopQ*, and *RipB* from *P. syringae*, *Xanthomonas* spp., and *Ralstonia* spp., respectively (Schultink et al. 2017; Thomas et al. 2020), but all 3 effectors are homologous and likely have nearly identical structures. *Pwl2* and *AVR<sub>a3</sub>* likely belong to effector families with different structural folds, suggesting that *MLA3* evolved to directly recognize 2 structurally distinct effectors. Comparing the structure and binding interfaces of *Pwl2* and *AVR<sub>a3</sub>*—once identified—will provide an initial step to elucidate the molecular mechanism of recognition. Despite having different overall structures, *AVR<sub>a3</sub>* and *Pwl2* might be directly recognized by *MLA3* due to a shared structural feature. This could represent a structural signature of pathogen effectors conserved across taxonomically diverse species and may guide effector discovery and NLR engineering toward expanded recognition and resistance.

## Materials and methods

### Plant materials and growth conditions

Barley (*H. vulgare*) accessions were obtained from United States Department of Agriculture Germplasm Resource Information Network (Aberdeen, ID, United States), Oregon State University (Corvallis, OR, United States), John Innes Centre (Norwich, United Kingdom), Wageningen University & Research (Wageningen, Netherlands), and CSIRO (Canberra, Australia). All barley accessions were subjected to single-seed descent before carrying out subsequent experiments. Barley growth conditions are listed in the relevant experimental sections. *E. curvula* was obtained from Star Seed, Inc. (Kansas, United States). *E. curvula* seedlings were grown in a Sanyo cabinet at 25 °C and 16-h photoperiod with a combination of 6 NVC NL/18/LED/T8/4/840 light bulbs and 9 NVC NL/18/LED/T8/4/865 light bulbs. *N. benthamiana* plants were grown in a controlled environment room at 22 °C, 80% humidity, and a 16-h light cycle provided by a combination of 6 Philips Master TL-D 58W/840 light

bulbs and 2 Sylvania GRO-LUX F58W/GRO-T8 fluorescent tubes.

### Recombination screen

Barley accessions Baronesse and BCD47 were crossed and allowed to self-pollinate to generate a founder  $F_2$  population. For the Baronesse  $\times$  BCD47 population, seedlings were germinated in John Innes Peat & Sand Mix (85% Fine Peat, 15% Grit, 2.7 kg/m<sup>3</sup> Osmocote 3 to 4 months, Wetting Agent, 4 kg/m<sup>3</sup> Maglime, and 1 kg PG Mix). Leaves were sampled at second leaf emergence, DNA extracted, and individuals genotyped for recombination events. Recombinants were transferred to larger pots in John Innes Cereal Mix (40% Medium Grade Peat, 40% Sterilized Soil, 20% Horticultural Grit, 1.3 kg/m<sup>3</sup> PG Mix 14-16-18 + Te Base Fertilizer, 1 kg/m<sup>3</sup> Osmocote Mini 16-8-11 2 mg + Te 0.02% B, Wetting Agent, 3 kg/m<sup>3</sup> Maglime, and 300 g/m<sup>3</sup> Exemptor) and grown in a greenhouse under natural daylight conditions.

Genetic markers designed for the barley oligonucleotide pool assay (BOPA1) panel were converted to KASP markers, which are also SNP based (Supplemental Data Set 3) (Close et al. 2009). Briefly, KASP SNP genotyping uses 2 competitive, allele-specific forward primers and 1 common reverse primer for allele-specific oligo extension, amplification, and fluorescence output. Genotyping was performed by the John Innes Centre Genotyping Facility (Norwich, United Kingdom). Genetic maps were created using JoinMap v4 that was used using default parameters (Van Ooijen 2006). Genetic distances were estimated using the Kosambi mapping function. Integrity of the genetic map was evaluated through comparison with the current OPA consensus genetic map of barley (Muñoz-Amatriaín et al. 2011) and using Rstudio (Version 1.1.463) and R/qtl package (Version 1.44.9) (Broman et al. 2003).

Recombination events in a 22.9 cM region on chromosome 1H including *Mla3* were identified in the Baronesse  $\times$  BCD47  $F_2$  population using a total of 1,152 individuals (2,304 gametes).

Marker saturation of the region encompassing *Mla* was performed using 12 KASP markers spanning a wide genetic interval from markers K\_3\_0933 to K\_4261. Twenty-four additional KASP markers were generated by identifying SNPs between Baronesse and BCD47 based on PCR amplification of the *Mla* locus. Following single-seed descent, DNA was extracted from leaf tissue of  $F_2$  and  $F_{2:3}$  recombinants using a CTAB-based protocol (Stewart and Via 1993). Briefly, 3 g of leaf tissue was ground on liquid N<sub>2</sub> and homogenized with 20 mL of CTAB extraction buffer (2% CTAB, 100 mM Tris-HCl pH 8.0, 20 mM EDTA pH 8.0, 1.4 M NaCl, and 1%  $\beta$ -mercaptoethanol). Samples were incubated for 30 min at 65 °C followed by 2 chloroform extractions and ethanol precipitation. DNA was then resuspended in 1 $\times$  TE and 50  $\mu$ g/mL Rnase A solution and incubated for 1 h at 37 °C. DNA was subsequently precipitated with 2.5 volumes of ice-cold 95% ethanol and resuspended in 1 $\times$  TE.

Quantification of DNA samples was performed using a NanoDrop spectrophotometer (Thermo Scientific) and the Qubit dsDNA HS Assay Kit (Molecular Probes, Life Technologies).

### RNA-seq and de novo transcriptome assembly

First and second leaf tissue was harvested at 10 d after sowing of barley accessions grown in the greenhouse under natural daylight conditions. Tissue was flash frozen in liquid nitrogen and stored at  $-80$  °C. Tissues were homogenized into a fine powder in liquid nitrogen-chilled pestle and mortars. RNA was extracted, purified, and quality assessed as described by Dawson et al. (2016). RNA libraries were constructed using Illumina TruSeq RNA library preparation (Illumina; RS-122-2001). Barcoded libraries were sequenced using either 100 or 150 bp paired-end reads. Library preparation and sequencing were performed by Earlham Institute (Norwich, United Kingdom), Novogene (Cambridge, United Kingdom), and BGI (Shenzhen, China). Quality of all RNA-seq data was assessed using FastQC (0.11.5). Trinity (2.4.0) (Grabherr et al. 2011) was used to assemble de novo transcriptomes using default parameters and Trimmomatic (Bolger et al. 2014) for read trimming. Genes of interest were identified in assemblies using BLAST+ (v2.2.9) (Camacho et al. 2009).

### Long-range assembly of Baronesse chromosome 1H

Long-range sequencing and assembly were carried out as described by Holden et al. (2022). Briefly, chromosome flow sorting of Baronesse chromosome 1H and preparation of its DNA were performed using the methods described by Doležel et al. (2012) with an estimated purity of 82.8% to 92.3% in the sorted fractions (Supplemental Fig. S12). Chromosomal high molecular weight (HMW) DNA, Chicago libraries and sequencing (Dovetail Genomics, Santa Cruz, CA, United States), assembly in Meraculous (v2.0.3), and final scaffolding in HiRise were performed as described in Thind et al. (2017). Shotgun sequencing was carried out using 2 insert sizes, estimated at 221 and 454 bp, with 266.3 and 246.9 million paired-end reads, respectively. An initial assembly using Meraculous had length 450.7 Mb on 40,855 scaffolds. The HiRise assembly had 454.5 Mb on 2,009 scaffolds.

### Sequence capture and PacBio SMRT sequencing

Sequence capture and PacBio SMRT sequencing of NLR encoding genes (RenSeq) were carried out according to Witek et al. (2016). A custom Daicel Arbor Biosciences Mybaits bait library was previously designed on the barley NLR gene space including the entire *Mla* locus from barley accession Morex (TSLMMHV1) (Brabham et al. 2018). PacBio circular consensus sequencing was performed at the Earlham Institute (Norwich, United Kingdom). De novo assembly was performed using Geneious (v10.2.3) using custom sensitivity parameters for assembly: don't merge variants with coverage over approximately 6, merge

homopolymer variants, allow gaps up to a maximum of 15% gaps per read, word length of 14, minimum overlap of 250 bp, ignore words repeated more than 200 times, 5% maximum mismatches per read, maximum gap size of 2, minimum overlap identity of 90%, index word length 12, reanalyze threshold of 8, and maximum ambiguity of 4.

### Copy number variation analysis

Copy number analysis was performed using the *k*-mer analysis toolkit (KAT; v.2.4.1) (Mapleson et al. 2017). The sequence coverage estimator tool (sect) was used to determine coverage for genomic contigs encompassing *Bpm*, *Mla3*, *RGH2*, and *RGH3*. Default parameters were used including *k*-mer length of 27 bp. *k*-medoids clustering was performed with R (4.1.2) using *pam* from the *cluster* package (2.1.3). Clustering was performed on coverage values between 0 and 1,000.

### Construct development

PCR amplifications were performed using GoTaq G2 Flexi DNA polymerase (Promega; Catalog number M7805), Phusion High Fidelity DNA polymerase (New England Biolabs Ltd; Catalog number M0530S), and GoTaq Long PCR Master Mix (Promega; Catalog number M4020). Reaction mixes were set up according to manufacturer's instructions and performed in a thermal cycler. cDNA was used as the template for cloning of the *RGH1* candidate genes, and gDNA was the template for the *RGH2* and *RGH3* constructs. Annealing temperatures and elongation times were optimized for reaction based on primer combination and ranged between 52 and 64 °C. PCRs were assayed on a 1% agarose gel in TBE or TAE buffer. Gel extraction of fragments was performed with the QIAquick gel extraction kit (Qiagen; Cat No.: 28704) according to the manufacturer's instructions. Excised and cleaned fragments were A-tailed via incubation at 72 °C for 20 min using GoTaq polymerase and dATPs, cloned via the TOPO XL PCR Cloning Kit (Invitrogen; K7030-20) according to manufacturer's instructions, and transformed into DH5α *Escherichia coli* competent cells (1 to 2 μL reaction into 50 μL cells). Transformations were placed on ice for 30 min, heat shocked at 42 °C for 90 s, placed on ice for 2 min, recovered in 500 μL L media via shaking at 37 °C for 1 h, and plated on L media plates in varying dilutions with appropriate selection for overnight growth at 37 °C. Positive clones were identified by PCR using gene-specific primers. Plasmids were extracted from positive colonies using 5 mL liquid cultures with the NucleoSpin Plasmid Purification kit (Macherey-Nagel; Ref.: 11932392) and sequenced (GATC; 80 to 100 ng/plasmid DNA, 5 μM primer). Plasmids were also confirmed through digestion with the restriction enzyme *EcoRI* (New England Biolabs; Ref.: R31015) according to the manufacturer's instructions. Presence of *Mla3Δ6* and differentiation between *Mla3* were assessed via digestion with *BspI* (Thermo Scientific; Cat No.: ER1151) which cuts on the 6 bp indel.

Plant transformation constructs were assembled via multiple PCR fragments into the pBract202 vector backbone. pBract202 was generated by the Crop Transformation (BRACT) team at the John Innes Centre (Norwich, United Kingdom) (Smedley and Harwood 2015). The backbone contains the *npt1* kanamycin resistance gene for bacterial selection, and the left border contains the 35S hygromycin selectable marker for plant transformation. Primers for Gibson Assembly consisted of 20 bp fusion from both fragments to be assembled (40 bp total) and were assessed for GC content (~50%) and secondary structures using mfold (Zuker 2003). Constructs were assembled via using Gibson Assembly (Gibson et al. 2009) with a Gibson Assembly master mix (New England Biolabs; Ref.: E2611). Briefly, multiple overlapping gene fragments are designed and amplified via PCR; appropriate overlaps are unique ~18 bp overhangs. Overlaps were added using the high-fidelity Phusion polymerase. PCR products were digested with *DpnI* (New England Biolabs; Ref.: R0176S) to remove circular DNA. Fragments were resolved with gel electrophoresis (1% agarose in 1× TAE buffer) and excised using the Zymoclean Gel DNA Recovery Kit (Zymo Research; Ref.: D4008) for elution of high-concentration ultrapure DNA. Fragments were added to the reaction tube in appropriate dilutions and ratios according to molecular weight, as outlined in the manufacturer's instructions. The reaction tube was incubated at 50 °C for 1 h—fragments trimmed by an exonuclease creating single-stranded 3' overhangs that anneal with their complementary counterparts, DNA polymerase extends 3' ends of annealed fragments, and sealed with a DNA ligase. Competent *E. coli* DH5α cells were transformed with the successful construct as outlined above. Construct visualization, primer development, and assessment were performed using the software Geneious (Version 9.0.5). Construct maps are shown in Supplemental Fig. S6.

### Plant transformation

Constructs were transformed into *Agrobacterium tumefaciens* AGL1 containing pSoup via electroporation (~100 ng plasmid into 50 μL cells), recovered in 500 μL L medium via shaking at 28 °C for 2 h, and grown on L media plates with appropriate selection for 3 d. Barley accession Golden Promise was transformed using *Agrobacterium*-mediated transformation based on the approach described by Hensel et al. (2009). Assessment of insert copy number of transgenic lines was performed by iDna Genetics Ltd (Norwich, United Kingdom) using real-time PCR assaying the presence of the hygromycin resistance gene.

### *B. graminis* propagation and inoculation

*Bgh* isolate CC148 was obtained from James Brown (John Innes Centre, Norwich, United Kingdom). Seedlings for phenotypic assays were germinated in John Innes Cereal Mix at 18 °C under a 16-h light and dark cycle. Seedlings were transferred to a containment greenhouse set at 18 °C day for 16 h and 12 °C night for 8 h with supplemental

lighting from 400W HQI (metal halide lamps). *Bgh* inoculations were carried out on seedlings at emergence of the second leaf. *Bgh* inoculum was maintained on the susceptible barley accession Manchuria. Inoculation was carried out by laying pots on their side and gently shaking infected leaves over both sides. Phenotyping was carried out as described in Bettgenhaeuser et al. (2021).

### *M. oryzae* propagation and inoculation

Protocols for culturing and inoculation of *M. oryzae* were similar as described by Jia et al. (2003) and Parker et al. (2008). *M. oryzae* isolates were maintained on potato dextrose agar medium at 24 °C and as frozen stocks of dried mycelium on Whatman filter paper (GE Healthcare Whatman Qualitative Filter Paper: Grade 1 Circles, Fisher Scientific UK) at –20 °C. Hyphal tips were transferred to oatmeal agar (20 g oatmeal, 10 g agar, 2.5 g sucrose, and addition of ddH<sub>2</sub>O to 500 mL) plates (deep petri dish 100 × 20 mm) for the production of spores (conidia) and incubated for 10 to 15 d at 24 °C. To increase spore production, plates were used for a second time after washing and a further 10- to 15-d incubation. For *M. oryzae* inoculation, seedlings were germinated in John Innes Cereal Mix (40% Medium Grade Peat, 40% Sterilized Soil, 20% Horticultural Grit, 1.3 kg/m<sup>3</sup> PG Mix 14-16-18 + Te Base Fertilizer, 1 kg/m<sup>3</sup> Osmocote Mini 16-8-11 2 mg + Te 0.02% B, Wetting Agent, 3 kg/m<sup>3</sup> Maglime, and 300 g/m<sup>3</sup> Exemptor). Seedlings were germinated and grown in a controlled environment at 25 °C under a 16-h light and dark cycle. *M. oryzae* conidia were collected by the addition of 8 mL dH<sub>2</sub>O to the oatmeal agar plates and gentle scraping with the tip of a 1.5-mL microcentrifuge tube. Suspension was poured and filtered through Miracloth (Merck Chemicals, Ref.: 475855-1r) and collected in a 50-mL Corning tube. Spore concentration was counted via hemocytometer and adjusted to 1 × 10<sup>5</sup> spores per milliliter in 0.1% gelatin or dH<sub>2</sub>O with 0.01% Tween 20 (Merck Chemicals, CAS Number: 9005-64-5).

*M. oryzae* spot inoculations were carried out on detached leaves on agar (2.5 g agar-agar [Fisher, CAS 9002-18-0]; 50 mL benzimidazole [1 g/1 L H<sub>2</sub>O stock solution]; 450 mL H<sub>2</sub>O). Barley was germinated at 25 °C under a 16-h light and dark cycle, and 1-wk-old seedlings were used for inoculation at emergence of second leaf. Barley was germinated in a Sanyo growth cabinet with the same conditions as listed for *E. curvula* growth above. The first leaf was cut and placed on agar inside the boxes. Each leaf was inoculated with 3 to 4 drops of 5 μL of conidial suspension. Boxes were placed at 25 °C in a Sanyo growth cabinet and maintained under continuous light for the first 24 h. After 24 h, droplets were removed from the leaves using sterile Miracloth and boxes returned to 25 °C in a 16-h light and dark cycle. Detached leaves were monitored for development of lesions, and phenotypes were recorded 7 d post inoculation (dpi). Phenotypes were scored as resistant on a scale of 0 = complete resistance; 1 = small brown resistant spots; 2 = susceptible larger eyespot lesions; 3 = larger spreading lesions; and 4 = hypersusceptibility.

*M. oryzae* spray inoculations were carried out on whole 1-wk-old seedlings at emergence of the second leaf. Barley was germinated 25 °C under a 16-h light and dark cycle with 9 seeds placed in a 9-cm<sup>2</sup> pot, with 8 pots in a tray. Each tray was sprayed with ~5 mL of conidial suspension using a 20-mm atomizer spray bottle. Trays were placed in polythene autoclave bags tied with tape and placed inside a Sanyo cabinet at 25 °C under a 16-h light and dark cycle. Bags remained covering the plants until phenotyping due to containment requirements. Disease symptoms were recorded 7 dpi, and first leaves scored on a similar phenotypic scale to spot inoculations. A similar protocol was followed for spray inoculations of 10-d-old weeping lovegrass (*E. curvula*) plants.

### *M. oryzae* mutagenesis

Mutagenesis of *M. oryzae* isolate KEN54-20 was performed on the conidial suspension using UV light. Spore concentration was adjusted to 1 × 10<sup>5</sup> spores per milliliter and placed inside a petri dish until the solution was just covering the entire base of the dish—a shallow depth is required to ensure even UV light penetration. The open petri dish was placed inside a UV Stratalinker 2400 (Stratagene) and exposed to set UV light. A dosage curve was generated to assess the UV dose at which spore death was at 50%; for KEN54-20, this was 20 s. The UV light-exposed conidial suspension was used for spray-based inoculation. Wild-type Baronesse was used for the isolation of KEN54-20 gain-of-virulence mutants. Lesions were isolated from leaves 7 dpi, sterilized in ethanol for 30 s, and placed on potato dextrose agar (10 g PDA, 6.25 g agar per liter of water). *M. oryzae* growth was sampled from each lesion, cultured, and reinoculated onto Baronesse to confirm gain of virulence.

### *M. oryzae* transformation

Transformation of *M. oryzae avr-Rmo1* isolates was performed as previously described (Talbot et al. 1993). Briefly, the region of fungal active growth was cut from the surface of a CM agar plate, blended in 50 mL of CM liquid media, and incubated for 48 h at 25 °C and 120 rpm. The culture was filtrated through 2 layers of sterile Miracloth, and mycelium was gently resuspended and digested with Glucanex in 0.7 M NaCl (pH 5.5, filter sterilized). Protoplasts were generated after incubation for 3 h at 25 °C and gentle shaking at 75 rpm. The digested mycelium was filtered through sterile Miracloth, and protoplasts were collected and centrifuged at 3,500 × g and 4 °C for 10 min. Protoplasts were washed with STC buffer (1.2 M sorbitol, 10 mM Tris-HCl pH 7.5, and 10 mM CaCl<sub>2</sub>), centrifuged at 3,500 × g for 10 min, and resuspended in 150 μL of STC buffer. Transformation was carried out by mixing the protoplasts with 4 μg of the vector pCB1532::pPWL2:PWL2:tPWL2, incubating at room temperature for 15 min, and subsequently adding 1 mL of PTC buffer (60% PEG 4000, 10 mM Tris-HCl pH 7.5, and 10 mM CaCl<sub>2</sub>). The mix was let to stand for 5 min at room temperature, added to BDCM liquid media (0.8 M sucrose, 1.7 g L-1 yeast nitrogen base without amino acids and ammonium sulfate, 2 g L-1 ammonium nitrate, 1 g L-1 asparagine, and 10 g L-1



glucose), and incubated overnight at 25 °C and 120 rpm. The protoplast culture was added to molten BDCM agar and poured onto plates. Selective BDCM medium (BDCM media lacking glucose) with 1% agar and sulfonyleurea (150 µg/mL chlorimuron ethyl) was added on top as overlay. Plates were incubated at 25 °C for 7 to 10 d until transformed colonies emerged and started to grow. Individual colonies were transferred to BDCM agar plates with 100 µg/mL sulfonyleurea and kept for confirmation by PCR and further assays.

### *M. oryzae* HMW genomic DNA extraction

HMW genomic DNA extraction from protoplasts of *M. oryzae* was performed for Oxford Nanopore DNA sequencing of the isolate KEN54-20. Protoplasts were obtained as previously described for *M. oryzae* transformation. Extraction of HMW DNA was carried out as previously described by Schwessinger and Rathjen (2017) with some modifications. Briefly, lysis buffer was prepared as follows: 2.5 volumes of autoclaved buffer A (0.35 M sorbitol, 0.1 M Tris-HCl, and 5 mM EDTA pH 8.0), 2.5 volumes of autoclaved buffer B (0.2 M Tris-HCl, 50 mM EDTA pH 8.0, 2 M NaCl, and 2% CTAB), 1 volume of filter-sterilized buffer C (5% sarkosyl *N*-lauroylsarcosine sodium salt), 1 volume of 10% PVP 40, 1 volume of 10% PVP 10, and 10 µL of RNase A (Thermo Fisher). Protoplasts were pelleted and thoroughly resuspended in preheated lysis buffer and incubated under constant rotation for 30 min at room temperature. Proteinase K (New England BioLabs) was added to the sample and further incubated under permanent rotation for 30 min, followed by 5 min on ice. The sample was mixed with 0.2 volumes of 5 M potassium acetate, incubated on ice for no longer than 5 min, and centrifuged at 4 °C and 5,000 × *g* for 12 min. The supernatant was transferred and mixed with 1 volume of phenol:chloroform:isoamyl alcohol (P:C:I) (25:24:1). After mixing by inversion for 2 min, the sample was centrifuged at 4 °C and 4,000 × *g* for 10 min. The supernatant was recovered and mixed once more with 1 volume of P:C:I, followed by centrifugation at 4 °C and 4,000 × *g* for 10 min to separate the organic phase and remove proteins. The supernatant was mixed by inversion with 0.1 volumes of 3 M sodium acetate, and then 1 volume of isopropanol was added. The sample was incubated at room temperature for 5 min and then centrifuged at 4 °C and 8,000 × *g* for 30 min. The supernatant was discarded, and the DNA, visible as a translucent pellet at the bottom, was washed with 70% ethanol and then centrifuged at 5,000 × *g* for 5 min. Four more additional washing steps with 70% ethanol were performed, with the final 2 spins at 13,000 × *g*. The ethanol was discarded, and the DNA pellet was let to air-dry for 5 min. The DNA was resuspended in molecular grade water and let to dissolve at room temperature. The sample was treated with RNase A (Thermo Fisher) and column purified using the Genomic DNA Clean and Concentrator Kit (Zymo Research) according to manufacturer's instructions. DNA concentration was measured using the Qubit dsDNA HS Assay Kit (Thermo Fisher).

### *M. oryzae* DNA sequencing

For genomic DNA Illumina sequencing, mycelia from 1-wk-old plates of *M. oryzae* isolates KEN54-20 and *avr-Rmo1* mutants were collected, ground with liquid nitrogen to a very fine powder, and transferred into 1.5-mL microcentrifuge tube until about two-thirds full. A total of 500 µL of CTAB buffer pH 7.5 (0.2 M Tris-HCl pH 7.5, 50 mM EDTA, 2 M NaCl, and 2% CTAB) was added, and samples were incubated at 65 °C for 30 min, shaking every 10 min. Subsequently, 500 µL of chloroform:isoamyl alcohol (24:1) was added, and samples were incubated for 30 min under constant shaking at 300 rpm, followed by centrifugation at 16,000 × *g* for 10 min. The aqueous phase (supernatant) was transferred into a new 1.5-mL microcentrifuge tube, and 500 µL of chloroform:isoamyl alcohol (24:1) was added, mixed for 5 min, and then centrifuged at 16,000 × *g* for 10 min. The top aqueous phase was transferred to a new tube, and 1 mL of ice-cold isopropanol was added and mixed. Samples were incubated at –20 °C for 2 h and then centrifuged at 16,000 × *g* for 10 min. The supernatants were discarded. DNA pellets were allowed to drain for 5 min and then completely resuspended in 500 µL of sterile water. A total of 50 µL of 3 M NaOAc was added with 1 mL of ice-cold 100% ethanol, followed by incubation at –20 °C for 1 h and centrifugation at 16,000 × *g* for 20 min. The supernatants were discarded, and 400 µL of ice-cold 70% ethanol was added. The samples were centrifuged at 16,000 × *g* for 5 min, the supernatants were discarded, and the pellets were allowed to air-dry. DNA samples were resuspended in 100 µL of TE + RNase A (Thermo Fisher) and stored at 4 °C. Concentrations of DNA samples were measured using the Qubit dsDNA HS Assay Kit (Thermo Fisher). DNA samples were submitted for library preparation and whole genome sequencing by Illumina to Novogene. The isolate KEN54-20 was sequenced with paired-end, 150 bp reads with libraries of 400 and 600 bp inserts, and KEN54-20 *avr-Rmo1* mutants were sequenced with paired-end, 150 bp reads with libraries of 400 bp inserts.

### Oxford Nanopore DNA sequencing

The gDNA library of *M. oryzae* KEN54-20 was prepared without shearing to maximize sequencing read length. Short DNA fragments were removed with the Short Read Eliminator Kit (Circuloromics) according to manufacturer's instructions. DNA repair, end-prep, adapter ligation, and clean-up were performed according to the 1D Lambda Control Experiment (SQK-LSK109) protocol provided by ONT. The library was loaded into an R9.4.1 FLO-MIN106 flow cell, and MinION sequencing was performed according to ONT guidelines using the ONT MinKNOW software.

### Genome assembly

Base calling of ONT sequencing data was performed with Guppy v3.2.2. Read quality assessment was performed using Pavy (https://github.com/conchoecia/pavy) and trimmed using NanoFilt (Li et al. 2009). The hybrid assembler MaSuRCA

v3.3.3 (Zimin et al. 2013) was used to assemble the reference genome of *M. oryzae* isolate KEN54-20 including ONT and Illumina data. Pilon (Walker et al. 2014) was used to improve the genome assembly. Alignment of Illumina reads to ONT data was performed using BWA (v0.7.12-r1039; <http://bio-bwa.sourceforge.net/>). Quality of the assembled and polished genome was assessed using the KAT (<https://github.com/TGAC/KAT>). Ab initio gene prediction was performed using Augustus (v3.3.2; <https://github.com/Gaius-Augustus/Augustus>) with the *M. oryzae* species gene model prediction. Genome assembly and annotation completeness were assessed with BUSCO v3 (Waterhouse et al. 2018). The *PWL2* region was investigated manually by aligning ONT reads to the reference genome using minimap2 (v2.17-r954-dirty). Illumina reads of *M. oryzae* KEN54-20 wild-type and *avr-Rmo1* mutants were aligned to the genome using BWA. Aligned reads were inspected using IGV (v2.5.3) (Robinson et al. 2011). The final assembly was 47.9 Mb on 39 contigs. A full set of commands is available on Github (<https://github.com/matthewmoscou/AvrRmo1>).

### Identification of common deletions in *M. oryzae avr-Rmo1* mutants

The KAT (v2.4.1) was used to scan the genome to identify *k*-mers ( $k = 27$ ) that were present in wild-type but absent in all *avr-Rmo1* mutants. A genome scan was performed by counting the number of *k*-mers present in wild type and absent in all mutants within a window of 10 kb with step size 1 kb.

### Molecular cloning for transient expression assays in *N. benthamiana*

The coding sequences of *Mla3* (UZM07847.1) and *Mla10* (AAQ55541.1) were domesticated to remove internal *BsaI* and *Bpil* restriction sites and were synthesized by Twist Bioscience (San Francisco, CA, United States). The synthesized gene fragments did not contain a stop codon and had *Bpil* external adapters for Golden Gate assembly into the acceptor plasmid pICSL01005 (TSL SynBio). For transient gene expression in *N. benthamiana*, each *Mla* allele was cloned into the binary acceptor plasmid pICH47732 (Addgene no. 4800) via Golden Gate assembly with pICH85281 (mannopine synthase +  $\Omega$  promoter [Mas  $\Omega$ ], Addgene no. 50272), pICSL50009 (6xHA C-terminal tag, Addgene no. 50309), and pICSL60008 (Arabidopsis heat shock protein terminator [AtHSP18 terminator], TSL SynBio). The *MLA3*<sup>L11E</sup> and *MLA10*<sup>L11E</sup> mutants were generated by site-directed mutagenesis through inverse PCR with the primer pairs *Mla3*<sub>L11E\_fw</sub> 5'-AAGAAGACAACGAGATTCCTCAAGTTGGGGAGCT-3' and *Mla3*<sub>L11E\_rv</sub> 5'-AAGAAGACAACTCGTTGGAAATGGCACCGGTGAC-3' and *Mla10*<sub>L11E\_fw</sub> 5'-AAGGTCTCACGAAATTCCAAAGTTGGGAGAATTG-3' and *Mla10*<sub>L11E\_rv</sub> 5'-AAGGTCTCATTCGTTAGAGATAGCACAGTAAC-3', respectively, using the binary constructs carrying the wild-type alleles as template. The PCR products were purified, digested with *BsaI* and religated.

The coding sequences of *PWL2* (AAA91019.1) and *AVR<sub>a10</sub>* (Saur et al. 2019) without signal peptide were domesticated to remove *Bpil* and *BsaI* restriction sites and synthesized and cloned by Twist Bioscience (San Francisco, CA, United States) with codon optimization for expression in *N. benthamiana*. The synthesized sequences were cloned without a stop codon in the pTwist\_Kan\_High\_Copy cloning vector (Twist Bioscience) with flanking *BsaI* restriction sites for subsequent Golden Gate assemblies. For transient gene expression in *N. benthamiana*, each effector was cloned into the binary acceptor plasmid pICH47732 (Addgene no. 4800) via Golden Gate assembly with pICH51266 (long 35S +  $\Omega$  promoter, Addgene no. 50267), pICSL50007 (3xFLAG C-terminal tag, Addgene no. 50308), and pICH41414 (35S terminator, Addgene no. 50337).

Each assembly was transformed into *E. coli* DH5 $\alpha$  for long-term storage, verified by DNA sequencing and subsequently transformed into *A. tumefaciens* GV3101::pMP90 for transient expression in planta.

### Transient gene expression in *N. benthamiana*

Transient gene expression in planta for cell death and coimmunoprecipitation assays was carried out by delivering T-DNA constructs transformed in *A. tumefaciens* GV3101::pMP90 into leaves of 4-wk-old *N. benthamiana* plants. Liquid cultures of LB medium inoculated with *A. tumefaciens* containing the constructs of interest were grown overnight at 28 °C under constant agitation. The cultures were centrifuged at 5,000  $\times$  g for 10 min, and cell pellets were resuspended in infiltration buffer (10 mM MES, 10 mM MgCl<sub>2</sub>, and 150  $\mu$ M acetosyringone). The OD<sub>600</sub> of each *A. tumefaciens* suspension was measured and adjusted to a final working concentration of 0.5 for MLA-HA expression constructs, 0.3 for *Pwl2*-FLAG, and 0.7 for *AVR<sub>a10</sub>*. The third and fourth upper leaves of 4-wk-old *N. benthamiana* plants were fully agroinfiltrated using a 1-mL disposable syringe. Leaves were collected 3 d after infiltration for protein extraction and coimmunoprecipitation. For cell death assays, the corresponding combinations of *A. tumefaciens* were also spot infiltrated on the third and fourth upper leaves of 4-wk-old *N. benthamiana* plants. Cell death phenotypes were recorded 3 d after infiltration.

### In planta coimmunoprecipitation assays

Two *N. benthamiana* leaves were harvested 3 d after agroinfiltration, frozen in liquid nitrogen, ground, and homogenized in a 1:2 w/v ratio with GTEN extraction buffer (10% glycerol, 25 mM Tris-HCl pH 7.5, 1 mM EDTA, and 300 mM NaCl) supplemented with 2% (w/v) PVPP, 10 mM DTT, 1% (v/v) protease inhibitor cocktail (Sigma), and 0.2% IGEPAL CA-630). Samples were centrifuged at 5,000  $\times$  g for 20 min at 4 °C, and the supernatant was transferred to a fresh tube and centrifuged under the same conditions for another 10 min. The supernatant was filtered through a Minisart 0.45- $\mu$ m filter to obtain the total protein extract (input). For coimmunoprecipitation assays, 1 mL of the total protein extract was mixed with 20  $\mu$ L of Anti-HA

Affinity Matrix from rat IgG1 (11815016001; Roche) or Anti-FLAG M2 Affinity Gel (A2220; Sigma-Aldrich) and incubated end over end for 1.5 h at 4 °C. Beads were washed 5 times with immunoprecipitation washing buffer (GTEN extraction buffer with 0.2% [v/v] IGEPAL CA-630) and resuspended in 60  $\mu$ L of 1 $\times$  Laemmli sample buffer (BioRad) supplemented with 10 mM DTT. Proteins were eluted from beads by incubating the samples at 80 °C for 10 min. Total protein extracts and immunoprecipitated samples were separated by SDS–PAGE and transferred onto a PVDF membrane using the Trans-Blot Turbo transfer system (BioRad) according to the manufacturer's instructions. Blots were incubated for 45 min in 5% (w/v) skim milk powder in 1 $\times$  TBST blocking solution. Epitope tag detection was performed with Anti-HA-Peroxidase, high-affinity antibody from rat IgG1 (12013819001; Roche), or ANTI-FLAG M2-Peroxidase (HRP) antibody produced in mouse (A8592; Sigma-Aldrich) in a 1:5,000 dilution in 5% (w/v) skim milk powder in 1 $\times$  TBST. Protein detection was done by adding Pierce ECL Western Blotting Substrate (Thermo Fisher Scientific) and SuperSignal West Femto Maximum Sensitivity Substrate (Thermo Fisher Scientific) in a 1:1 (v/v) ratio. Membrane imaging was performed using an Amersham ImageQuant 800 western blot imager system. Protein loading was checked by staining the blots with Ponceau S solution (Sigma).

### Phylogenetic analysis of grass NLRs

To identify NLRs from diverse grass species (Supplemental Data Set 4), InterProScan v5.36-75.0 using default parameters was used to annotate individual protein domains. Proteins annotated with the NB domain Pfam family (PF00931) were identified and individual domains extracted from NLRs using the Python script QKdomain\_process.py (Bailey et al. 2018). Structure-guided multiple sequence alignment of NB domains was performed with MAFFT (v7.481) using DASH (default parameters). NB structures included in the alignment were derived from *A. thaliana* ZAR1 (PDB 6J5T) and *S. lycopersicum* (tomato) NRC1 (PDB 6S2P). The QKphylogeny\_alignment\_analysis.py Python script was used to filter the alignment for variable sites represented in at least 40% of proteins and sequences spanning at least 50% of the alignment length (<https://github.com/matthewmoscou/QKphylogeny>). The phylogenetic tree was constructed using RAxML (v8.2.12) with the JTT amino acid substitution model, gamma model of rate heterogeneity, and 1,000 bootstraps. A convergence test performed using RAxML autoMRE found convergence for both the full NB and C17 clade after 250 bootstraps. iTOL was used for phylogenetic tree visualization, and *A. thaliana* ZAR1 was used as outgroups. Alignments and machine-readable tree files are available on the figshare repository.

### Accession numbers

The RNA-seq data used in this study are found in the NCBI database under BioProject codes PRJNA292371,

PRJNA376252, PRJNA378334, and PRJNA378723. The genome assembly and sequencing data for barley accession Baronesse chromosome 1H generated in this study have been deposited in the NCBI database under BioProject code PRJNA879438. RenSeq-PacBio of Baronesse raw, circular consensus sequences, and de novo assembly have been deposited in the NCBI database under BioProject code PRJNA422986. Genomic sequencing data and assembly for *M. oryzae* isolate KEN54-20 and *avr-rmo1* have been deposited in the NCBI database under BioProject code PRJNA881958. The sequences of plasmids used for plant transformation in this study have been deposited in the NCBI database with accession codes OP561810 (*Mla3*), OP561809 (*Mla3Δ6*), and OP561811 (*RGH2/RGH3*). All data needed to evaluate the conclusions in the paper are present in the paper and/or the Supplemental data. Raw genotypic, phenotypic, and source data for figures and supplemental figures have been deposited on figshare (<https://doi.org/10.6084/m9.figshare.21365532.v2>). A material transfer agreement with The Sainsbury Laboratory is required to receive the materials. The use of the materials will be limited to noncommercial research uses only. Please contact M.J.M. (matthew.moscou@usda.gov) regarding biological materials, and requests will be responded to within 60 d.

### Acknowledgments

We greatly appreciate valuable discussions with Sebastian Schornack, Sophien Kamoun, Isabel Saur, Takaki Maekawa, and Paul Schulze-Lefert. Genotyping was supported by Richard Goram (John Innes Centre genotyping facility). Photography was supported by Andrew Davis and Phil Robinson. Assistance in the greenhouse was provided by Sue Banfield and the John Innes Centre Horticultural team. Seed was provided by Rients Niks, Wendy Harwood, Patrick Hayes, Wolfgang Spielmeyer, Roger Wise, and the National Small Grains Collection (USDA-ARS). We thank P. Cápál, M. Said, Z. Dubská, J. Weiserová, and E. Jahnová (Institute of Experimental Botany, Olomouc) for assistance with chromosome flow sorting and preparation of chromosome DNA.

### Author contributions

Conceptualization: M.J.M. Data curation: M.J.M. Formal analysis: H.J.B., D.G.D.L.C., and M.J.M. Funding acquisition: M.J.M., R.T., N.J.T., J.D., K.S., and T.W. Investigation: H.J.B., D.G.D.L.C., V.W., J.R., I.H.-P., P.G., J.L., M.Sh., K.F., H.Š., I.M., H.S., J.T., and M.Sm. Methodology: M.Sh., H.S., Y.K.G., and H.J.B. Project administration: M.J.M. Resources: K.S., V.W., N.J.T., and R.T. Software: M.J.M. Supervision: M.Sh., K.F., H.S., K.S., J.D., Y.K.G., T.W., N.J.T., R.T., and M.J.M. Validation: V.W., J.R., and N.J.T. Visualization: H.J.B., D.G.D.L.C., and M.J.M. Writing—original draft: H.J.B., D.G.D.L.C., and M.J.M. Writing—review and editing: H.J.B., D.G.D.L.C., and M.J.M.

## Supplemental data

The following materials are available in the online version of this article.

**Supplemental Figure S1.** Genomic regions flanking the *Mla* locus are conserved between barley accessions Morex and Baronesse.

**Supplemental Figure S2.** *k*-mer coverage distribution for *Bpm*, *Mla3*, and *RGH2/RGH3*.

**Supplemental Figure S3.** Barley accessions carrying identical *RGH2* and *RGH3* alleles in Baronesse are susceptible to *M. oryzae* KEN54-20.

**Supplemental Figure S4.** Barley accessions carrying *Mla3* and *Mla23* are resistant to *M. oryzae* KEN54-20.

**Supplemental Figure S5.** *MLA3* and *MLA23* are closely related *RGH1* (*MLA*) alleles.

**Supplemental Figure S6.** Transformation constructs for *Rmo1* candidate genes.

**Supplemental Figure S7.** *avr-Rmo1* mutants are virulent on Baronesse.

**Supplemental Figure S8.** Genome-wide scan of regions with modified sequence relative to *M. oryzae* isolate Ken54-20.

**Supplemental Figure S9.** The L11E mutation in *MLA3* and *MLA10* impairs their cell death inducing activity.

**Supplemental Figure S10.** Structure-guided phylogenetic tree of NLR NB domain from several PACMAD grasses.

**Supplemental Figure S11.** PACMAD grasses lack an ortholog of the *RGH1* (*MLA*) gene family.

**Supplemental Figure S12.** Flow cytometric analysis and sorting of barley cv. Baronesse chromosome 1H for long-range sequencing.

**Supplemental Data Set 1.** De novo assembled barley leaf transcriptomes.

**Supplemental Data Set 2.** Inventory of transgenic barley lines with *Mla3*, *Mla3Δ6*, *RGH2/RGH3*.

**Supplemental Data Set 3.** KASP markers used for fine mapping of the *Mla3/Rmo1* locus.

**Supplemental Data Set 4.** Genomes used for NLR phylogenetic tree construction.

## Funding

Funding for this research includes United Kingdom Research and Innovation-Biotechnology and Biological Sciences Research Council Norwich Research Park Doctoral Training Partnership (grant no. BB/M011216/1 to JR) and Institute Strategic Programme (grant no. BB/P012574/1 to M.J.M. and BBS/E/J/000 PR9795 to M.J.M.), European Regional Development Fund (grant no. CZ.02.1.01/0.0/0.0/16\_019/0000827 to I.M., J.D., and H.Š.), Perry Foundation (H.J.B.), Japan Society for the Promotion of Science 2018 Summer Programme (H.J.B.), Gatsby Charitable Foundation (M.J.M. and N.J.T.), and United States Department of Agriculture-Agricultural Research Service CRIS #5062-21220-025-000D (M.J.M.).

*Conflict of interest statement.* None declared.

## References

- Adachi H, Contreras MP, Harant A, Wu C-H, Derevnina L, Sakai T, Duggan C, Moratto E, Bozkurt TO, Maqbool A, et al.** An N-terminal motif in NLR immune receptors is functionally conserved across distantly related plant species. *eLife* 2019;**8**:e49956. <https://doi.org/10.7554/eLife.49956>
- Ahn H-K, Lin X, Olave-Achury AC, Derevnina L, Contreras MP, Kourelis J, Wu C-H, Kamoun S, Jones JDG.** Effector-dependent activation and oligomerization of plant NRC class helper NLRs by sensor NLR immune receptors *Rpi-amr3* and *Rpi-amr1*. *EMBO J*. 2023;**42**(5):e111484. <https://doi.org/10.15252/embj.2022111484>
- Ashfield T, Ong LE, Nobuta K, Schneider CM, Innes RW.** Convergent evolution of disease resistance gene specificity in two flowering plant families. *Plant Cell* 2004;**16**(2):309–318. <https://doi.org/10.1105/tpc.016725>
- Ashfield T, Redditt T, Russell A, Kessens R, Rodibaugh N, Galloway L, Kang Q, Podicheti R, Innes RW.** Evolutionary relationship of disease resistance genes in soybean and Arabidopsis specific for the *Pseudomonas syringae* effectors *AvrB* and *AvrRpm1*. *Plant Physiol*. 2014;**166**(1):235–251. <https://doi.org/10.1104/pp.114.244715>
- Axtell MJ, Staskawicz BJ.** Initiation of RPS2-specified disease resistance in Arabidopsis is coupled to the *AvrRpt2*-directed elimination of RIN4. *Cell* 2003;**112**(3):369–377. [https://doi.org/10.1016/S0092-8674\(03\)00036-9](https://doi.org/10.1016/S0092-8674(03)00036-9)
- Bailey PC, Schudoma C, Jackson W, Baggs E, Dagdas G, Haerty W, Moscou M, Krasileva KV.** Dominant integration locus drives continuous diversification of plant immune receptors with exogenous domain fusions. *Genome Biol*. 2018;**19**(1):23. <https://doi.org/10.1186/s13059-018-1392-6>
- Bauer S, Yu D, Lawson AW, Saur IM, Frantzeskakis L, Kracher B, Logemann E, Chai J, Maekawa T, Schulze-Lefert P.** The leucine-rich repeats in allelic barley *MLA* immune receptors define specificity towards sequence-unrelated powdery mildew avirulence effectors with a predicted common RNase-like fold. *PLoS Pathog*. 2021;**17**(2):e1009223. <https://doi.org/10.1371/journal.ppat.1009223>
- Bennetzen JL, Schmutz J, Wang H, Percifield R, Hawkins J, Pontaroli AC, Estep M, Feng L, Vaughn JN, Grimwood J, et al.** Reference genome sequence of the model plant *Setaria*. *Nat Biotechnol*. 2012;**30**(6):555–561. <https://doi.org/10.1038/nbt.2196>
- Bettgenhaeuser J, Hernández-Pinzón I, Dawson AM, Gardiner M, Green P, Taylor J, Smoker M, Ferguson JN, Emmrich P, Hubbard A.** The barley immune receptor *Mla* recognizes multiple pathogens and contributes to host range dynamics. *Nat Commun*. 2021;**12**(1):6915. <https://doi.org/10.1038/s41467-021-27288-3>
- Bilgic H, Steffenson B, Hayes P.** Molecular mapping of loci conferring resistance to different pathotypes of the spot blotch pathogen in barley. *Phytopathology* 2006;**96**(7):699–708. <https://doi.org/10.1094/PHYTO-96-0699>
- Bolger AM, Lohse M, Usadel B.** Trimmomatic: a flexible trimmer for Illumina sequence data. *Bioinformatics* 2014;**30**(15):2114–2120. <https://doi.org/10.1093/bioinformatics/btu170>
- Bourras S, Kunz L, Xue M, Praz CR, Müller MC, Kälin C, Schläfli M, Ackermann P, Flückiger S, Parlange F.** The *AvrPm3*-*Pm3* effector-NLR interactions control both race-specific resistance and host-specificity of cereal mildews on wheat. *Nat Commun*. 2019;**10**(1):2292. <https://doi.org/10.1038/s41467-019-10274-1>
- Bourras S, Praz CR, Spanu PD, Keller B.** Cereal powdery mildew effectors: a complex toolbox for an obligate pathogen. *Curr Opin Microbiol*. 2018;**46**:26–33. <https://doi.org/10.1016/j.mib.2018.01.018>
- Brabham HJ, Hernández-Pinzón I, Holden S, Lorang J, Moscou MJ.** An ancient integration in a plant NLR is maintained as a trans-species polymorphism. *bioRxiv* 239541. <https://doi.org/10.1101/239541>, 08 January 2018, preprint: not peer reviewed.
- Briggs FN, Stanford EH.** Linkage of factors for resistance to mildew in barley. *J Genet*. 1938;**37**(1):107–117. <https://doi.org/10.1007/BF02982145>

- Broman KW, Wu H, Sen Š, Churchill GA.** R/qlt: QTL mapping in experimental crosses. *Bioinformatics* 2003;**19**(7):889–890. <https://doi.org/10.1093/bioinformatics/btg112>
- Brown JK, Tellier A.** Plant-parasite coevolution: bridging the gap between genetics and ecology. *Annu Rev Phytopathol.* 2011;**49**: 345–367. <https://doi.org/10.1146/annurev-phyto-072910-095301>
- Caldwell KS, Michelmore RW.** *Arabidopsis thaliana* genes encoding defense signaling and recognition proteins exhibit contrasting evolutionary dynamics. *Genetics* 2009;**181**(2):671–684. <https://doi.org/10.1534/genetics.108.097279>
- Camacho C, Coulouris G, Avagyan V, Ma N, Papadopoulos J, Bealer K, Madden TL.** BLAST+: architecture and applications. *BMC Bioinformatics* 2009;**10**:421. <https://doi.org/10.1186/1471-2105-10-421>
- Cao Y, Kümmel F, Logemann E, Gebauer JM, Lawson AW, Yu D, Uthoff M, Keller B, Jirschtzka J, Baumann U, et al.** Structural polymorphisms within a common powdery mildew effector scaffold as a driver of co-evolution with cereal immune receptors. *bioRxiv* 2023.2005.2005.539654. <https://doi.org/10.1101/2023.05.05.539654>, 08 May 2023, preprint: not peer reviewed.
- Carballo J, Santos BACM, Zappacosta D, Garbus I, Selva JP, Gallo CA, Díaz A, Albertini E, Caccamo M, Echenique V.** A high-quality genome of *Eragrostis curvula* grass provides insights into Poaceae evolution and supports new strategies to enhance forage quality. *Sci Rep.* 2019;**9**(1):10250. <https://doi.org/10.1038/s41598-019-46610-0>
- Carter ME, Helm M, Chapman AV, Wan E, Restrepo Sierra AM, Innes RW, Bogdanove AJ, Wise RP.** Convergent evolution of effector protease recognition by *Arabidopsis* and barley. *Mol Plant Microbe Interact.* 2019;**32**(5):550–565. <https://doi.org/10.1094/MPMI-07-18-0202-FI>
- Cesari S.** Multiple strategies for pathogen perception by plant immune receptors. *New Phytol.* 2018;**219**(1):17–24. <https://doi.org/10.1111/nph.14877>
- Cesari S, Bernoux M, Moncuquet P, Kroj T, Dodds PN.** A novel conserved mechanism for plant NLR protein pairs: the “integrated decoy” hypothesis. *Front Plant Sci.* 2014;**5**:606. <https://doi.org/10.3389/fpls.2014.00606>
- Chen J, Upadhyaya NM, Ortiz D, Sperschneider J, Li F, Bouton C, Breen S, Dong C, Xu B, Zhang X.** Loss of AvrSr50 by somatic exchange in stem rust leads to virulence for Sr50 resistance in wheat. *Science* 2017;**358**(6370):1607–1610. <https://doi.org/10.1126/science.aao4810>
- Close TJ, Bhat PR, Lonardi S, Wu Y, Rostoks N, Ramsay L, Druka A, Stein N, Svensson JT, Wanamaker S.** Development and implementation of high-throughput SNP genotyping in barley. *BMC Genomics* 2009;**10**:582. <https://doi.org/10.1186/1471-2164-10-582>
- Contreras MP, Pai H, Tumtas Y, Duggan C, Yuen ELH, Cruces AV, Kourelis J, Ahn H-K, Lee K-T, Wu C-H, et al.** Sensor NLR immune proteins activate oligomerization of their NRC helpers in response to plant pathogens. *EMBO J.* 2023;**42**(5):e111519. <https://doi.org/10.15252/embj.2022111519>
- Cooley MB, Pathirana S, Wu H-J, Kachroo P, Klessig DF.** Members of the *Arabidopsis* HRT/RPP8 family of resistance genes confer resistance to both viral and oomycete pathogens. *Plant Cell* 2000;**12**(5): 663–676. <https://doi.org/10.1105/tpc.12.5.663>
- Couch BC, Kohn LM.** A multilocus gene genealogy concordant with host preference indicates segregation of a new species, *Magnaporthe oryzae*, from *M. grisea*. *Mycologia* 2002;**94**(4): 683–693. <https://doi.org/10.1080/15572536.2003.11833196>
- Dangl JL, Jones JD.** Plant pathogens and integrated defence responses to infection. *Nature* 2001;**411**(6839):826–833. <https://doi.org/10.1038/35081161>
- Dawson AM, Ferguson JN, Gardiner M, Green P, Hubbard A, Moscou MJ.** Isolation and fine mapping of Rps6: an intermediate host resistance gene in barley to wheat stripe rust. *Theor Appl Genet.* 2016;**129**(4):831–843. <https://doi.org/10.1007/s00122-015-2659-x>
- de Guillen K, Ortiz-Vallejo D, Gracy J, Fournier E, Kroj T, Padilla A.** Structure analysis uncovers a highly diverse but structurally conserved effector family in phytopathogenic fungi. *PLoS Pathog.* 2015;**11**(10):e1005228. <https://doi.org/10.1371/journal.ppat.1005228>
- Ding J, Zhang W, Jing Z, Chen J-Q, Tian D.** Unique pattern of R-gene variation within populations in *Arabidopsis*. *Mol Genet Genomics.* 2007;**277**(6):619–629. <https://doi.org/10.1007/s00438-007-0213-5>
- Doležel J, Vrána J, Šafář J, Bartoš J, Kubaláková M, Šimková H.** Chromosomes in the flow to simplify genome analysis. *Funct Integr Genomics.* 2012;**12**(3):397–416. <https://doi.org/10.1007/s10142-012-0293-0>
- Flor H.** The complementary genic systems in flax and flax rust. *Adv Genet.* 1956;**8**:29–54. [https://doi.org/10.1016/S0065-2660\(08\)60498-8](https://doi.org/10.1016/S0065-2660(08)60498-8)
- Franceschetti M, Maqbool A, Jimenez-Dalmaroni MJ, Pennington HG, Kamoun S, Banfield MJ.** Effectors of filamentous plant pathogens: commonalities amid diversity. *Microbiol Mol Biol Rev.* 2017;**81**(2):2. <https://doi.org/10.1128/MMBR.00066-16>
- Fujisaki K, Abe Y, Ito A, Saitoh H, Yoshida K, Kanzaki H, Kanzaki E, Utsushi H, Yamashita T, Kamoun S.** Rice Exo70 interacts with a fungal effector, AVR-Pii, and is required for AVR-Pii-triggered immunity. *Plant J.* 2015;**83**(5):875–887. <https://doi.org/10.1111/tpj.12934>
- Gibson DG, Young L, Chuang R-Y, Venter JC, Hutchison CA, Smith HO.** Enzymatic assembly of DNA molecules up to several hundred kilobases. *Nat Methods.* 2009;**6**(5):343–345. <https://doi.org/10.1038/nmeth.1318>
- Gladioux P, Condon B, Ravel S, Soanes D, Maciel JLN, Nhani Jr A, Chen L, Terauchi R, Lebrun M-H, Tharreau D.** Gene flow between divergent cereal-and grass-specific lineages of the rice blast fungus *Magnaporthe oryzae*. *MBio* 2018;**9**(1):e01219-01217. <https://doi.org/10.1128/mBio.01219-17>
- Goff SA, Ricke D, Lan T-H, Presting G, Wang R, Dunn M, Glazebrook J, Sessions A, Oeller P, Varma H, et al.** A draft sequence of the rice genome *Oryza sativa* L. ssp. (*japonica*). *Science* 2002;**296**(5565): 92–100. <https://doi.org/10.1126/science.1068275>
- Goggin FL, Jia L, Shah G, Hebert S, Williamson VM, Ullman DE.** Heterologous expression of the Mi-1.2 gene from tomato confers resistance against nematodes but not aphids in eggplant. *Mol Plant Microbe Interact.* 2006;**19**(4):383–388. <https://doi.org/10.1094/MPMI-19-0383>
- Grabherr MG, Haas BJ, Yassour M, Levin JZ, Thompson DA, Amit I, Adiconis X, Fan L, Raychowdhury R, Zeng Q.** Trinity: reconstructing a full-length transcriptome without a genome from RNA-Seq data. *Nat Biotechnol.* 2011;**29**(7):644–652. <https://doi.org/10.1038/nbt.1883>
- Halterman D, Wise RP.** A single-amino acid substitution in the sixth leucine-rich repeat of barley MLA6 and MLA13 alleviates dependence on RAR1 for disease resistance signaling. *Plant J.* 2004;**38**(2): 215–226. <https://doi.org/10.1111/j.1365-313X.2004.02032.x>
- Halterman D, Zhou F, Wei F, Wise RP, Schulze-Lefert P.** The MLA6 coiled-coil, NBS-LRR protein confers AvrMla6-dependent resistance specificity to *Blumeria graminis* f. sp. *hordei* in barley and wheat. *Plant J.* 2001;**25**(3):335–348. <https://doi.org/10.1046/j.1365-313x.2001.00982.x>
- Helm M, Qi M, Sarkar S, Yu H, Whitham SA, Innes RW.** Engineering a decoy substrate in soybean to enable recognition of the soybean mosaic virus Nla protease. *Mol Plant Microbe Interact.* 2019;**32**(6): 760–769. <https://doi.org/10.1094/mpmi-12-18-0324-r>
- Hensel G, Kastner C, Oleszczuk S, Riechen J, Kumlehn J.** Agrobacterium-mediated gene transfer to cereal crop plants: current protocols for barley, wheat, triticale, and maize. *Int J Plant Genomics.* 2009;**2009**:835608. <https://doi.org/10.1155/2009/835608>
- Holden S, Bergum M, Green P, Bettgenhaeuser J, Hernández-Pinzón I, Thind A, Clare S, Russell JM, Hubbard A, Taylor J.** A lineage-specific Exo70 is required for receptor kinase-mediated immunity in barley. *Sci Adv.* 2022;**8**(27):eabn7258. <https://doi.org/10.1126/sciadv.abn7258>

- Holm L. Dali server: structural unification of protein families. *Nucleic Acids Res.* 2022;**50**(W1):W210–W215. <https://doi.org/10.1093/nar/gkac387>
- Huang J, Si W, Deng Q, Li P, Yang S. Rapid evolution of avirulence genes in rice blast fungus *Magnaporthe oryzae*. *BMC Genet.* 2014;**15**:45. <https://doi.org/10.1186/1471-2156-15-45>
- Inoue Y, Vy TT, Yoshida K, Asano H, Mitsuoka C, Asuke S, Anh VL, Cumagun CJ, Chuma I, Terauchi R. Evolution of the wheat blast fungus through functional losses in a host specificity determinant. *Science* 2017;**357**(6346):80–83. <https://doi.org/10.1126/science.aam9654>
- Inukai T, Vales MI, Hori K, Sato K, Hayes PM. RMo 1 confers blast resistance in barley and is located within the complex of resistance genes containing Mla, a powdery mildew resistance gene. *Mol Plant Microbe Interact.* 2006;**19**(9):1034–1041. <https://doi.org/10.1094/MPMI-19-1034>
- Jacob S. *Magnaporthe oryzae*: Methods and Protocols. New York (NY): Springer; 2021.
- Jia Y, McAdams SA, Bryan GT, Hershey HP, Valent B. Direct interaction of resistance gene and avirulence gene products confers rice blast resistance. *EMBO J.* 2000;**19**(15):4004–4014. <https://doi.org/10.1093/emboj/19.15.4004>
- Jia Y, Valent B, Lee F. Determination of host responses to *Magnaporthe grisea* on detached rice leaves using a spot inoculation method. *Plant Disease* 2003;**87**(2):129–133. <https://doi.org/10.1094/PDIS.2003.87.2.129>
- Jones JD, Dangl JL. The plant immune system. *Nature* 2006;**444**(7117):323–329. <https://doi.org/10.1038/nature05286>
- Jørgensen JH, Wolfe M. Genetics of powdery mildew resistance in barley. *CRC Crit Rev Plant Sci.* 1994;**13**(1):97–119. <https://doi.org/10.1080/07352689409701910>
- Jumper J, Evans R, Pritzel A, Green T, Figurnov M, Ronneberger O, Tunyasuvunakool K, Bates R, Židek A, Potapenko A. Highly accurate protein structure prediction with AlphaFold. *Nature* 2021;**596**(7873):583–589. <https://doi.org/10.1038/s41586-021-03819-2>
- Kang S, Swegard JA, Valent B. The PWL host specificity gene family in the blast fungus *Magnaporthe grisea*. *Mol Plant Microbe Interact.* 1995;**8**(6):939–948. <https://doi.org/10.1094/MPMI-8-0939>
- Kim H-S, Desveaux D, Singer AU, Patel P, Sonddek J, Dangl JL. The *Pseudomonas syringae* effector AvrRpt2 cleaves its C-terminally acylated target, RIN4, from *Arabidopsis* membranes to block RPM1 activation. *Proc Natl Acad Sci U S A.* 2005;**102**(18):6496–6501. <https://doi.org/10.1073/pnas.0500792102>
- Kim MG, Geng X, Lee SY, Mackey D. The *Pseudomonas syringae* type III effector AvrRpm1 induces significant defenses by activating the *Arabidopsis* nucleotide-binding leucine-rich repeat protein RPS2. *Plant J.* 2009;**57**(4):645–653. <https://doi.org/10.1111/j.1365-313X.2008.03716.x>
- Kim SH, Qi D, Ashfield T, Helm M, Innes RW. Using decoys to expand the recognition specificity of a plant disease resistance protein. *Science* 2016;**351**(6274):684–687. <https://doi.org/10.1126/science.aad3436>
- Kinizios S, Jahoor A, Fischbeck G. Powdery-mildew-resistance genes Mla29 and Mla32 in *H. spontaneum* derived winter-barley lines. *Plant Breeding* 1995;**114**(3):265–266. <https://doi.org/10.1111/j.1439-0523.1995.tb00809.x>
- Kølster P, Stølen O. Barley isolines with genes for resistance to *Erysiphe graminis* f. sp. *hordei* in the recurrent parent ‘Siri’. *Plant Breeding* 1987;**98**(1):79–82. <https://doi.org/10.1111/j.1439-0523.1987.tb01096.x>
- Kourelis J, van der Hoorn RAL. Defended to the nines: 25 years of resistance gene cloning identifies nine mechanisms for R protein function. *Plant Cell* 2018;**30**(2):285–299. <https://doi.org/10.1105/tpc.17.00579>
- Kuang H, Caldwell KS, Meyers BC, Michelmore RW. Frequent sequence exchanges between homologs of RPP8 in *Arabidopsis* are not necessarily associated with genomic proximity. *Plant J.* 2008;**54**(1):69–80. <https://doi.org/10.1111/j.1365-313X.2008.03408.x>
- Lai Y, Eulgem T. Transcript-level expression control of plant NLR genes. *Mol Plant Pathol.* 2018;**19**(5):1267–1281. <https://doi.org/10.1111/mpp.12607>
- Leng Y, Zhao M, Fiedler J, Dreiseitl A, Chao S, Li X, Zhong S. Molecular mapping of loci conferring susceptibility to spot blotch and resistance to powdery mildew in barley using the sequencing-based genotyping approach. *Phytopathology* 2020;**110**(2):440–446. <https://doi.org/10.1094/PHYTO-08-19-0292-R>
- Leng Y, Zhao M, Wang R, Steffenson BJ, Brueggeman RS, Zhong S. The gene conferring susceptibility to spot blotch caused by *Cochliobolus sativus* is located at the Mla locus in barley cultivar Bowman. *Theor Appl Genet.* 2018;**131**(7):1531–1539. <https://doi.org/10.1007/s00122-018-3095-5>
- Le Roux C, Huet G, Jauneau A, Camborde L, Trémoussaygue D, Kraut A, Zhou B, Levailant M, Adachi H, Yoshioka H. A receptor pair with an integrated decoy converts pathogen disabling of transcription factors to immunity. *Cell* 2015;**161**(5):1074–1088. <https://doi.org/10.1016/j.cell.2015.04.025>
- Lewis JD, Lee AH-Y, Hassan JA, Wan J, Hurley B, Jhingree JR, Wang PW, Lo T, Youn J-Y, Guttman DS. The *Arabidopsis* ZED1 pseudokinase is required for ZAR1-mediated immunity induced by the *Pseudomonas syringae* type III effector HopZ1a. *Proc Natl Acad Sci U S A.* 2013;**110**(46):18722–18727. <https://doi.org/10.1073/pnas.1315520110>
- Li H, Handsaker B, Wysoker A, Fennell T, Ruan J, Homer N, Marth G, Abecasis G, Durbin R. The sequence alignment/map format and SAMtools. *Bioinformatics* 2009;**25**(16):2078–2079. <https://doi.org/10.1093/bioinformatics/btp352>
- Li Z, Huang J, Wang Z, Meng F, Zhang S, Wu X, Zhang Z, Gao Z. Overexpression of *Arabidopsis* nucleotide-binding and leucine-rich repeat genes RPS2 and RPM1(D505V) confers broad-spectrum disease resistance in rice. *Front Plant Sci.* 2019;**10**:417. <https://doi.org/10.3389/fpls.2019.00417>
- Lu X, Kracher B, Saur IM, Bauer S, Ellwood SR, Wise R, Yaeno T, Maekawa T, Schulze-Lefert P. Allelic barley MLA immune receptors recognize sequence-unrelated avirulence effectors of the powdery mildew pathogen. *Proc Natl Acad Sci U S A.* 2016;**113**(42):E6486–E6495. <https://doi.org/10.1073/pnas.1612947113>
- Ma Y, Guo H, Hu L, Martinez PP, Moschou PN, Cevik V, Ding P, Duxbury Z, Sarris PF, Jones JD. Distinct modes of derepression of an *Arabidopsis* immune receptor complex by two different bacterial effectors. *Proc Natl Acad Sci U S A.* 2018;**115**(41):10218–10227. <https://doi.org/10.1073/pnas.1811858115>
- Mackey D, Belkadir Y, Alonso JM, Ecker JR, Dangl JL. *Arabidopsis* RIN4 is a target of the type III virulence effector AvrRpt2 and modulates RPS2-mediated resistance. *Cell* 2003;**112**(3):379–389. [https://doi.org/10.1016/S0092-8674\(03\)00040-0](https://doi.org/10.1016/S0092-8674(03)00040-0)
- Mackey D, Holt BF III, Wiig A, Dangl JL. RIN4 interacts with *Pseudomonas syringae* type III effector molecules and is required for RPM1-mediated resistance in *Arabidopsis*. *Cell.* 2002;**108**(6):743–754. [https://doi.org/10.1016/S0092-8674\(02\)00661-X](https://doi.org/10.1016/S0092-8674(02)00661-X)
- Maekawa T, Kracher B, Saur IM, Yoshikawa-Maekawa M, Kellner R, Pankin A, von Korff M, Schulze-Lefert P. Subfamily-specific specialization of RGH1/MLA immune receptors in wild barley. *Mol Plant Microbe Interact.* 2019;**32**(1):107–119. <https://doi.org/10.1094/MPMI-07-18-0186-FI>
- Mapleson D, Garcia Accinelli G, Kettleborough G, Wright J, Clavijo BJ. KAT: a K-mer analysis toolkit to quality control NGS datasets and genome assemblies. *Bioinformatics* 2017;**33**(4):574–576. <https://doi.org/10.1093/bioinformatics/btw663>
- Märkle H, Saur IML, Stam R. Evolution of resistance (R) gene specificity. *Essays Biochem.* 2022;**66**(5):551–560. <https://doi.org/10.1042/ebc20210077>
- Masaki HI, de Villiers S, Qi P, Prado K, Kaimenyi DK, Tesfaye K, Alemu T, Takan J, Dida M, Ringo J, et al. Host specificity controlled

- by *PWL1* and *PWL2* effector genes in the finger millet blast pathogen *Magnaporthe oryzae* in eastern Africa. *Mol Plant Microbe Interact.* 2023;**36**(9):584–591. <https://doi.org/10.1094/mpmi-01-23-0012-r>
- Mascher M, Wicker T, Jenkins J, Plott C, Lux T, Koh CS, Ens J, Gundlach H, Boston LB, Tulpová Z.** Long-read sequence assembly: a technical evaluation in barley. *Plant Cell* 2021;**33**(6):1888–1906. <https://doi.org/10.1093/plcell/koab077>
- Mazo-Molina C, Mainiero S, Haefner BJ, Bednarek R, Zhang J, Feder A, Shi K, Strickler SR, Martin GB.** *Ptr1* evolved convergently with *RPS2* and *Mrs5* to mediate recognition of *AvrRpt2* in diverse solanaceous species. *Plant J.* 2020;**103**(4):1433–1445. <https://doi.org/10.1111/tpj.v103.4>
- McDowell JM, Dhandaydham M, Long TA, Aarts MG, Goff S, Holub EB, Dangl JL.** Intragenic recombination and diversifying selection contribute to the evolution of downy mildew resistance at the *RPP8* locus of *Arabidopsis*. *Plant Cell* 1998;**10**(11):1861–1874. <https://doi.org/10.1105/tpc.10.11.1861>
- Mukhi N, Brown H, Gorenkin D, Ding P, Bentham AR, Stevenson CE, Jones JD, Banfield MJ.** Perception of structurally distinct effectors by the integrated WRKY domain of a plant immune receptor. *Proc Natl Acad Sci U S A.* 2021;**118**(50):e2113996118. <https://doi.org/10.1073/pnas.2113996118>
- Muñoz-Amatrián M, Moscou MJ, Bhat PR, Svensson JT, Bartoš J, Suchánková P, Šimková H, Endo TR, Fenton RD, Lonardi S.** An improved consensus linkage map of barley based on flow-sorted chromosomes and single nucleotide polymorphism markers. *Plant Genome.* 2011;**4**(3):238–249. <https://doi.org/10.3835/plantgenome2011.08.0023>
- Ngou BPM, Ding P, Jones JDG.** Thirty years of resistance: zig-zag through the plant immune system. *Plant Cell* 2022;**34**(5):1447–1478. <https://doi.org/10.1093/plcell/koac041>
- Nombela G, Williamson VM, Muñoz M.** The root-knot nematode resistance gene *Mi-1.2* of tomato is responsible for resistance against the whitefly *Bemisia tabaci*. *Mol Plant Microbe Interact.* 2003;**16**(7):645–649. <https://doi.org/10.1094/MPMI.2003.16.7.645>
- Ortiz D, Chen J, Outram MA, Saur IML, Upadhyaya NM, Mago R, Ericsson DJ, Cesari S, Chen C, Williams SJ, et al.** The stem rust effector protein *AvrSr50* escapes *Sr50* recognition by a substitution in a single surface-exposed residue. *New Phytol.* 2022;**234**(2):592–606. <https://doi.org/10.1111/nph.18011>
- Ou SH.** Rice diseases. 2nd ed. Slough: CAB International; 1985.
- Parker D, Beckmann M, Enot DP, Overy DP, Rios ZC, Gilbert M, Talbot N, Draper J.** Rice blast infection of *Brachypodium distachyon* as a model system to study dynamic host/pathogen interactions. *Nat Protoc.* 2008;**3**(3):435–445. <https://doi.org/10.1038/nprot.2007.499>
- Paterson AH, Bowers JE, Bruggmann R, Dubchak I, Grimwood J, Gundlach H, Haberer G, Hellsten U, Mitros T, Poliakov A, et al.** The *Sorghum bicolor* genome and the diversification of grasses. *Nature* 2009;**457**(7229):551–556. <https://doi.org/10.1038/nature07723>
- Pariyannan S, Moore J, Ayliffe M, Bansal U, Wang X, Huang L, Deal K, Luo M, Kong X, Bariana H.** The gene *Sr33*, an ortholog of barley *Mla* genes, encodes resistance to wheat stem rust race Ug99. *Science* 2013;**341**(6147):786–788. <https://doi.org/10.1126/science.1239028>
- Prokhorchik M, Choi S, Chung E-H, Won K, Dangl JL, Sohn KH.** A host target of a bacterial cysteine protease virulence effector plays a key role in convergent evolution of plant innate immune system receptors. *New Phytol.* 2020;**225**(3):1327–1342. <https://doi.org/10.1111/nph.16218>
- Ravensdale M, Nemri A, Thrall PH, Ellis JG, Dodds PN.** Co-evolutionary interactions between host resistance and pathogen effector genes in flax rust disease. *Mol Plant Pathol.* 2011;**12**(1):93–102. <https://doi.org/10.1111/j.1364-3703.2010.00657.x>
- Robinson JT, Thorvaldsdóttir H, Winckler W, Guttman M, Lander ES, Getz G, Mesirov JP.** Integrative genomics viewer. *Nat Biotechnol.* 2011;**29**(1):24–26. <https://doi.org/10.1038/nbt.1754>
- Russell AR, Ashfield T, Innes RW.** *Pseudomonas syringae* effector *AvrPphB* suppresses *AvrB*-induced activation of *RPM1* but not *AvrRpm1*-induced activation. *Mol Plant Microbe Interact.* 2015;**28**(6):727–735. <https://doi.org/10.1094/MPMI-08-14-0248-R>
- Santos D, Martins da Silva P, Abrantes I, Maleita C.** Tomato *Mi-1.2* gene confers resistance to *Meloidogyne luci* and *M. ethiopica*. *Eur J Plant Pathol.* 2020;**156**(2):571–580. <https://doi.org/10.1007/s10658-019-01907-8>
- Sarris PF, Duxbury Z, Huh SU, Ma Y, Segonzac C, Sklenar J, Derbyshire P, Cevik V, Rallapalli G, Saucet SB.** A plant immune receptor detects pathogen effectors that target WRKY transcription factors. *Cell* 2015;**161**(5):1089–1100. <https://doi.org/10.1016/j.cell.2015.04.024>
- Saucet SB, Ma Y, Sarris PF, Furzer OJ, Sohn KH, Jones JD.** Two linked pairs of *Arabidopsis* TNL resistance genes independently confer recognition of bacterial effector *AvrRps4*. *Nat Commun.* 2015;**6**:6338. <https://doi.org/10.1038/ncomms7338>
- Saur IML, Bauer S, Kracher B, Lu X, Franzeskakis L, Müller MC, Sabelleck B, Kimmel F, Panstruga R, Maekawa T, et al.** Multiple pairs of allelic *MLA* immune receptor-powdery mildew *AVRA* effectors argue for a direct recognition mechanism. *eLife* 2019;**8**:e44471. <https://doi.org/10.7554/eLife.44471>
- Saur IML, Panstruga R, Schulze-Lefert P.** NOD-like receptor-mediated plant immunity: from structure to cell death. *Nat Rev Immunol.* 2021;**21**(5):305–318. <https://doi.org/10.1038/s41577-020-00473-z>
- Schnable PS, Ware D, Fulton RS, Stein JC, Wei F, Pasternak S, Liang C, Zhang J, Fulton L, Graves TA, et al.** The B73 maize genome: complexity, diversity, and dynamics. *Science* 2009;**326**(5956):1112–1115. <https://doi.org/10.1126/science.1178534>
- Schneider D, Saraiva A, Azzoni A, Miranda H, de Toledo M, Pelloso A, Souza A.** Overexpression and purification of *PWL2D*, a mutant of the effector protein *PWL2* from *Magnaporthe grisea*. *Protein Expr Purif.* 2010;**74**(1):24–31. <https://doi.org/10.1016/j.pep.2010.04.020>
- Schultink A, Qi T, Lee A, Steinbrenner AD, Staskawicz B.** *Roq1* mediates recognition of the *Xanthomonas* and *Pseudomonas* effector proteins *XopQ* and *HopQ1*. *Plant J.* 2017;**92**(5):787–795. <https://doi.org/10.1111/tpj.2017.92.issue-5>
- Schwinger B, Rathjen JP.** Wheat rust diseases. New York (NY): Springer; 2017.
- Seeholzer S, Tsuchimatsu T, Jordan T, Bieri S, Pajonk S, Yang W, Jahoor A, Shimizu KK, Keller B, Schulze-Lefert P.** Diversity at the *Mla* powdery mildew resistance locus from cultivated barley reveals sites of positive selection. *Mol Plant Microbe Interact.* 2010;**23**(4):497–509. <https://doi.org/10.1094/MPMI-23-4-0497>
- Seong K, Krasileva K.** Comparative computational structural genomics highlights divergent evolution of fungal effectors. *bioRxiv.* <https://doi.org/10.1101/2022.05.02.490317>, 02 May 2022, preprint: not peer reviewed.
- Seto D, Koulena N, Lo T, Menna A, Guttman DS, Desveaux D.** Expanded type III effector recognition by the *ZAR1* NLR protein using *ZED1*-related kinases. *Nat Plants.* 2017;**3**(4):1–4. <https://doi.org/10.1038/nplants.2017.27>
- Shen Q-H, Zhou F, Bieri S, Haizel T, Shirasu K, Schulze-Lefert P.** Recognition specificity and *RAR1/SGT1* dependence in barley *Mla* disease resistance genes to the powdery mildew fungus. *Plant Cell* 2003;**15**(3):732–744. <https://doi.org/10.1105/tpc.009258>
- Sirisathaworn T, Srirat T, Longya A, Jantasuriyarat C.** Evaluation of mating type distribution and genetic diversity of three *Magnaporthe oryzae* avirulence genes, *PWL-2*, *AVR-Pii* and *Avr-Piz-t*, in Thailand rice blast isolates. *Agric Nat Resour.* 2017;**51**(1):7–14. <https://doi.org/10.1016/j.anres.2016.08.005>
- Smedley MA, Harwood WA.** Agrobacterium protocols. New York (NY): Springer; 2015.
- Stewart CN, Via LE.** A rapid CTAB DNA isolation technique useful for RAPD fingerprinting and other PCR applications. *Biotechniques* 1993;**14**(5):748–751.
- Sun J, Huang G, Fan F, Wang S, Zhang Y, Han Y, Zou Y, Lu D.** Comparative study of *Arabidopsis* *PBS1* and a wheat *PBS1* homolog

- helps understand the mechanism of PBS1 functioning in innate immunity. *Sci Rep*. 2017;7(1):5487. <https://doi.org/10.1038/s41598-016-0028-x>
- Sweigard JA, Carroll AM, Kang S, Farrall L, Chumley FG, Valent B.** Identification, cloning, and characterization of PWL2, a gene for host species specificity in the rice blast fungus. *Plant Cell* 1995;7(8):1221–1233. <https://doi.org/10.1105/tpc.7.8.1221>
- Takahashi H, Miller J, Nozaki Y, Takeda M, Shah J, Hase S, Ikegami M, Ehara Y, Dinesh-Kumar S, Sukamto.** RCY1, an *Arabidopsis thaliana* RPP8/HRT family resistance gene, conferring resistance to cucumber mosaic virus requires salicylic acid, ethylene and a novel signal transduction mechanism. *Plant J*. 2002;32(5):655–667. <https://doi.org/10.1046/j.1365-313X.2002.01453.x>
- Talbot NJ, Ebbole DJ, Hamer JE.** Identification and characterization of MPG1, a gene involved in pathogenicity from the rice blast fungus *Magnaporthe grisea*. *Plant Cell* 1993;5(11):1575–1590. <https://doi.org/10.1105/tpc.5.11.1575>
- Thind AK, Wicker T, Šimková H, Fossati D, Moullet O, Brabant C, Vrána J, Doležel J, Krattinger SG.** Rapid cloning of genes in hexaploid wheat using cultivar-specific long-range chromosome assembly. *Nat Biotechnol*. 2017;35(8):793–796. <https://doi.org/10.1038/nbt.3877>
- Thomas NC, Hendrich CG, Gill US, Allen C, Hutton SF, Schultink A.** The immune receptor Roq1 confers resistance to the bacterial pathogens *Xanthomonas*, *Pseudomonas syringae*, and *Ralstonia* in TomatoData\_Sheet\_1.pdf. *Front Plant Sci*. 2020;11. <https://doi.org/10.3389/fpls.2020.00463>
- Valent B, Crawford MS, Weaver CG, Chumley FG.** Genetic studies of fertility and pathogenicity in *Magnaporthe grisea* (*Pyricularia oryzae*). *Iowa State J. Res*. 1986;60(4):569–594.
- Van Der Biezen EA, Jones JD.** Plant disease-resistance proteins and the gene-for-gene concept. *Trends Biochem Sci*. 1998;23(12):454–456. [https://doi.org/10.1016/S0968-0004\(98\)01311-5](https://doi.org/10.1016/S0968-0004(98)01311-5)
- Van der Hoorn RA, De Wit PJ, Joosten MH.** Balancing selection favors guarding resistance proteins. *Trends Plant Sci*. 2002;7(2):67–71. [https://doi.org/10.1016/S1360-1385\(01\)02188-4](https://doi.org/10.1016/S1360-1385(01)02188-4)
- Van Ooijen J.** Joinmap 4. Software for the calculation of genetic linkage maps in experimental populations. Vol. 33. Wageningen, Netherlands: Kyazma BV; 2006.
- Vogel JP, Garvin DF, Mockler TC, Schmutz J, Rokhsar D, Bevan MW, Barry K, Lucas S, Harmon-Smith M, Lail K, et al.** Genome sequencing and analysis of the model grass *Brachypodium distachyon*. *Nature* 2010;463(7282):763–768. <https://doi.org/10.1038/nature08747>
- Vos P, Simons G, Jesse T, Wijbrandi J, Heinen L, Hogers R, Frijters A, Groenendijk J, Diergaarde P, Reijans M, et al.** The tomato Mi-1 gene confers resistance to both root-knot nematodes and potato aphids. *Nat Biotechnol*. 1998;16(13):1365–1369. <https://doi.org/10.1038/4350>
- Walker BJ, Abeel T, Shea T, Priest M, Abouelliel A, Sakthikumar S, Cuomo CA, Zeng Q, Wortman J, Young SK, et al.** Pilon: an integrated tool for comprehensive microbial variant detection and genome assembly improvement. *PLoS One* 2014;9(11):e112963. <https://doi.org/10.1371/journal.pone.0112963>
- Wang G, Roux B, Feng F, Guy E, Li L, Li N, Zhang X, Lautier M, Jardinaud M-F, Chabannes M.** The decoy substrate of a pathogen effector and a pseudokinase specify pathogen-induced modified-self recognition and immunity in plants. *Cell Host Microbe*. 2015;18(3):285–295. <https://doi.org/10.1016/j.chom.2015.08.004>
- Wang X, Richards J, Gross T, Druka A, Kleinhofs A, Steffenson B, Acevedo M, Brueggeman R.** The rpg4-mediated resistance to wheat stem rust (*Puccinia graminis*) in barley (*Hordeum vulgare*) requires Rpg5, a second NBS-LRR gene, and an actin depolymerization factor. *Mol Plant Microbe Interact*. 2013;26(4):407–418. <https://doi.org/10.1094/MPMI-06-12-0146-R>
- Waterhouse RM, Seppely M, Simão FA, Manni M, Ioannidis P, Klioutchnikov G, Kriventseva EV, Zdobnov EM.** BUSCO applications from quality assessments to gene prediction and phylogenomics. *Mol Biol Evol*. 2018;35(3):543–548. <https://doi.org/10.1093/molbev/msx319>
- Wei F, Gobelman-Werner K, Morroll SM, Kurth J, Mao L, Wing R, Leister D, Schulze-Lefert P, Wise RP.** The Mla (powdery mildew) resistance cluster is associated with three NBS-LRR gene families and suppressed recombination within a 240-kb DNA interval on chromosome 5S (1HS) of barley. *Genetics* 1999;153(4):1929–1948. <https://doi.org/10.1093/genetics/153.4.1929>
- Wei F, Wing RA, Wise RP.** Genome dynamics and evolution of the Mla (powdery mildew) resistance locus in barley. *Plant Cell* 2002;14(8):1903–1917. <https://doi.org/10.1105/tpc.002238>
- Williams SJ, Sohn KH, Wan L, Bernoux M, Sarris PF, Segonzac C, Ve T, Ma Y, Saucet SB, Ericsson DJ.** Structural basis for assembly and function of a heterodimeric plant immune receptor. *Science* 2014;344(6181):299–303. <https://doi.org/10.1126/science.1247357>
- Witek K, Jupe F, Witek AI, Baker D, Clark MD, Jones JD.** Accelerated cloning of a potato late blight-resistance gene using RenSeq and SMRT sequencing. *Nat Biotechnol*. 2016;34(6):656–660. <https://doi.org/10.1038/nbt.3540>
- Zhang X, Dodds PN, Bernoux M.** What do we know about NOD-like receptors in plant immunity? *Annu Rev Phytopathol*. 2017;55(1):205–229. <https://doi.org/10.1146/phyto.2017.55.issue-1>
- Zhou F, Kurth J, Wei F, Elliott C, Valè G, Yahiaoui N, Keller B, Somerville S, Wise R, Schulze-Lefert P.** Cell-autonomous expression of barley Mla1 confers race-specific resistance to the powdery mildew fungus via a Rar1-independent signaling pathway. *Plant Cell*. 2001;13(2):337–350. <https://doi.org/10.1105/tpc.13.2.337>
- Zimin AV, Marçais G, Puiu D, Roberts M, Salzberg SL, Yorke JA.** The MaSuRCA genome assembler. *Bioinformatics* 2013;29(21):2669–2677. <https://doi.org/10.1093/bioinformatics/btt476>
- Zuker M.** Mfold web server for nucleic acid folding and hybridization prediction. *Nucleic Acids Res*. 2003;31(13):3406–3415. <https://doi.org/10.1093/nar/gkg595>